JPRS-UPM-92-006
9 November 1992

JPRS Report

Science & Technology

Central Eurasia: Physics & Mathematics

Science & Technology
Central Eurasia: Physics & Mathematics

JPRS-UPM-92-006 *9 November 1992*

CONTENTS

NUCLEAR PHYSICS

OPTICS, SPECTROSCOPY

PLASMA PHYSICS

SUPERCONDUCTIVITY

THEORETICAL PHYSICS

High-Conducting State in Thin Polymer Films. Effect of Electric Field and Uniaxial Pressure

927J0270D Moscow ZHURNAL EKSPERIMENTALNOY I TEORETICHESKOY FIZIKI in Russian Vol 102 No 1(7), Jul 92 pp 187-193

[Article by A. N. Lachinov, A. Yu. Zherebov, V. M. Kornilov, Bashkir Scientific Center at the Urals Department of Russia's Academy of Sciences]

[Abstract] The newly discovered high-conducting state (VPS) in undoped unconjugated polypropylene- and polydiphenylphthalide-type polymers (PDF) and the origin of the abnormally high conductivity measured in thin polymer films are discussed. The outcome of an experimental investigation into abnormally high conductivity of thin polymer films induced by an electric field and a low uniaxial pressure and the mutual effect of these two factors on the formation of the high-conducting state is presented. PDF films produced by centrifuging from a solution in cyclohexanol are used in the study whereby a three-layer film sandwich structure with metal layers on the outside (Cu, Al, Au, Cr, or In) is produced. The upper layer is either sprayed or rolled onto the polymer layer. The dependence of the current through a 0.4 μm thick polymer film on the uniaxial pressure and the voltage-current characteristics of a thin polymer film in the initial dielectric and intermediate states and under a 0.4 MPa pressure as well as the voltage-current characteristic of a film under a 0.1 MPa pressure and a bipolar sawtooth voltage at a 0.1 Hz frequency an a 10 V amplitude are plotted. The findings demonstrate that the mechanism of high-conducting state with a metal-like temperature dependence of conductivity is electronic in origin. The origin of the high conductivity domains (or conducting channels) is not fully ascertained and it is speculated that they represent areas of peak trap density whereby the trap ionization facilitated by the electric field leads to the development of charged states. Figures 3; references 17: 9 Russian, 8 Western.

New Matrix Memory' Manifestations Under Dye Molecule Absorption by Nonuniform Surface

927J0274B St. Petersburg PISMA V ZHURNAL TEKHNICHESKOY FIZIKI in Russian Vol 18 No 11, Jun 92 pp 27-30

[Article by V. N. Berger; UDC 02; 11]

[Abstract] Matrix memory—a phenomenon whereby the difference in the electron absorption and fluorescence spectra of the adsorbates produced by saturating porous glass from the solutions of the same dye in different solvents is preserved for a long time—is discussed and a new manifestation of matrix memory is discovered and reported. In essence, the integral light absorption cross section and the magnitude of the fluorescence quantum yield of the adsorbed molecules' ensemble depend on the type of solvent used to inject the dye into porous glass and this dependence is maintained after the solvent is removed from the pores. The dependence of the integral light absorption cross section of various dyes adsorbed by the molecules on Henry's constant (at 293K) of the solvent is plotted. The findings are consistent with the matrix memory phenomena reported and explained earlier. It is noted that the results reflect the changes in the integral absorption cross section within the entire absorption band. Measurements produce the same results when the porous glass thickness is manipulated in the experiment within a 2-0.5 mm range. The author is grateful to A.V. Sechkarev for discussions and interest in the effort. Figures 1; references 4.

New Features of Physical Properties of Blue Liquid Crystal Phases

927J0278B St. Petersburg PISMA V ZHURNAL TEKHNICHESKOY FIZIKI in Russian Vol 18 No 9, May 92 pp 43-48

[Article by O. G. Vlokh, Yu. A. Nastishin, T. M. Sosnovskiy, Lvov State University imeni I. Franko; UDC 03; 12]

[Abstract] Manifestations of three-dimensional translational ordering in the blue phases (BP) of liquid crystals (ZhK) whereby the substance viscosity increases sharply in these phases are discussed and the temperature dependence of dynamic viscosity of cholesterylpelargonate (KhP), temperature dependence of electric conductivity of cholesterylpelargonate+nonioxybenzoic acid (NOBK) at various applied voltages, temperature hysteresis of electric conductivity of the KhP+NOBK mixture, the behavior of optical activity in the blue phase, and temperature hysteresis loops of optical activity in the blue phase are plotted. An experimental study shows that there are no $\sigma(T)$ anomalies in the blue phases if the applied voltage is less than the critical voltage of electrohydrodynamic instability (EGD) in the cholesteric phase (Ch) and is manifested as shallow minima above the critical voltage. The appearance of EGD flows leads to a sharp increase in conductivity while the disappearance of EGD flows does not lead to a noticeable conductivity drop. The temperature hysteresis loops attest to a blue phase overcooling whereby the overcooled condition is remarkably stable to external factors. The optical activity behavior at a constant temperature attests to the blue phase metastability while the unusual robustness of the metastable state is attributed to the viscous friction of the superstructure, local structure, and impurity defects in the blue phase. The existence of a superstructure in the blue phase structure is alleged. Figures 2; references 5: 3 Russian, 2 Western.

On Solitons With Small Number of Time or Space Periods

937J0008A Moscow VESTNIK MOSKOVSKOGO UNIVERSITETA: SERIYA 3, FIZIKA ASTRONOMIYA in Russian Vol 33 No 3, May-Jun 92 pp 4-20

[Article by A. V. Vederko, O. B. Dubrovskaya, V. F. Marchenko, A. P. Sukhorukov, Moscow University; UDC 621.3.09:621.373.1]

[Abstract] The development and propagation of solitons—pulses which preserve their shape due to a balance of dispersive and nonlinear effects—in media of various physical origins and the methods generally used to describe envelope solitons away from resonance and critical frequencies, such as the nonlinear Schroedinger equation (NUSh) method, are outlined. Several new classes of solitons which differ in principle from regular envelope solitons are discussed. These primarily include solitons with a small number of field oscillations as a result of which the wave packet concept is not applicable and it is therefore necessary to use the method of slowly changing profile, just as in nonlinear optics. The use of this method leads to a modified Korteweg-deVries equation (mKdF). The soliton and breezer propagation is considered and it is shown that as the number of periods increases, a breezer converts into an envelope soliton. The principal properties of solitons near the critical frequencies at which the group velocity is equal to zero are considered and it is shown that nonpropagating solitons can be excited near the critical frequencies and that color or three-frequency solitons can be excited in the continuous phase. The theory and numerical simulation of solitons with a small number of space or time periods in a media with dispersion and nonlinearity described by Duffing's equation are examined. The slow soliton generation and propagation and a cubic-nonlinear medium with a bounded transmission band is illustrated in a waveguide and a periodic structure. Precise analytical soliton equations are derived and the soliton domain is identified. Slow soliton excitation conditions in a nonlinear medium are investigated. Figures 11; references 23: 15 Russian, 8 Western.

Stimulated Emission Dynamics Analysis of Ti-Doped Sapphire Laser Under Double Mode Locking and Limited Ultrashort Pump Pulse Train

937J0017A Minsk ZHURNAL PRIKLADNOY SPEKTROSKOPII in Russian Vol 57 No 1-2, Jul-Aug 92 pp 75-81

[Article by M. I. Demchuk, V. L. Kalashnikov, V. P. Kalosha, V. P. Mikhaylov, Scientific Research Institute of Physical Problems imeni A.N. Sevchenko at the Belarussian State University imeni V.I. Lenin, Minsk; UDC 621.378.3:541.651]

[Abstract] Stimulated emission capabilities of Ti-doped sapphire lasers (Al_2O_3:Ti^{3+}) are discussed and stimulated emission of a limited picosecond pulse train-pumped Ti-doped sapphire laser under mode locking using a saturable passive gate, i.e., double mode locking, is investigated in order to ascertain the effect of the pumping and gate parameters on the possibility of shortening the stimulated emission ultrashort pulse (UKI) duration. The study is based on analyzing the stimulated emission pulse behavior during multiple stimulated radiation transmission through an amplifying medium, a spectral filter, a saturable absorber, and output mirror which make up the laser cavity, starting with the arrival of the first pump pulse. A system of coupling equations which corresponds to the study model is derived; the train-average lasing pulse duration as a function of the saturation parameter under mode locked pumping, the train-average lasing pulse and satellite intensity and stimulated emission delay as a function of the saturation parameter under mode-locked pumping, the mean lasing train duration and intensity as a function of the peak pump train intensity and length, and the mean lasing pulse and satellite duration and intensity as a function of the pump detuning and saturation parameter are plotted. An analysis shows that ultrashort pulse lasing in the system under study differs from that of dye lasers by a more than 100 ns delay in the lasing train maximum relative to the pump train maximum. The delay decreases with power. It is shown that by selecting the optimum absorber saturation parameters, one can shorten a lasing pulse duration to a value limited by the filter even at a limited pump pulse train whereby the pump detuning and a transition to multiple pumping have a significant effect on the optimum saturation parameter. Figures 6; references 16: 9 Russian, 7 Western.

Spectral Structure of Au-Vapor Laser's 312.2 nm Line

937J0017B Minsk ZHURNAL PRIKLADNOY SPEKTROSKOPII in Russian Vol 57 No 1-2, Jul-Aug 92 pp 87-91

[Article by L. V. Gorchakov, G. S. Yevtushenko, Atmospheric Optics Institute at the Siberian Department of Russia's Academy of Sciences, Tomsk; UDC 621.378.33]

[Abstract] The hyperfine structure (STS) of the ultraviolet emission of a gold vapor laser at a 312.2 nm wavelength is discussed and the results of a calculation of the Doppler line shape of the 312.2 nm line allowing for the hyperfine structure are presented. A formula is derived for calculating the individual level energy in the hyperfine structure and the constants *A, B* of certain Au atom levels and shifts and relative component intensities of the 312.2 nm line are summarized. The hyperfine structure of certain gold levels, the allowed transitions between the hyperfine component levels of the 312.2 nm line, the relative positions of the hyperfine structure components and their intensities, and the Doppler line shape (allowing for the hyperfine structure) and the behavior of its half-width with an increase in temperature are plotted. A lower stimulated emission spectrum half-width relative to the spontaneous emission half-width is noted; it is attributed to the fact that the total active medium saturation condition has not been attained and the principal contribution to lasing is made by the most intensive components; as a result, it is possible to reach a relatively narrow ($\leq$0.05 cm^{-1}) ultraviolet lasing line by lowering the operating temperature or using an unstable cavity. Figures 4; tables 2; references 10: 4 Russian, 6 Western.

Nonlinear Modes of Generation of Longitudinal Sound Pulses in Piezoelectric Cell by Ultrashort Laser Action

927J0276A Moscow AKUSTICHESKIY ZHURNAL in Russian Vol 38 No 4, Jul-Aug 92 (manuscript received 28 Jun 91) pp 683-692

[Article by V. E. Gusev and L. N. Makarova, Moscow State University imeni M. V. Lomonosov; UDC 535.211:621.315]

[Abstract] Generation of longitudinal sound pulses in a piezoelectric crystal with a photoelectric effect upon its nonlinear with respect to light intensity excitation by ultrashort laser pulses is analyzed theoretically, such sound pulses being generated by the reverse piezoelectric effect as photoelectrons and photoholes become spatially segregated owing to their different mobility and thus set up an electric field which deforms the crystal. The longitudinal deformation profile outside the generation region is described as a function of time $\tau = t - z/c_L$ in a system of coordinates which travels with the sound at its velocity c_L, assuming that the crystal extends infinitely deep below its free surface $z = 0$ and considering that the mode of optoacoustic energy conversion depends on the depth of light penetration into the crystal. First is considered the case of a small light penetration depth and correspondingly a thin light-absorbing layer within which electric charges will segregate so that an electric field distribution will evolve, this distribution becoming steady after a transient period whose length is of the order of the Maxwell electron-distribution relaxation time $T_{M,e}$. In this case one can regard photoexcitation of electron-hole pairs as a superficial process and describe the propagation of electron-hole plasma accordingly.

When now the electron diffusion velocity is much lower than the speed of sound (ratio of sound travel time to electron diffusion time $m << 1$) so that finiteness of the light penetration depth cannot be disregarded, then the electron drift velocity remains much lower than the electron diffusion velocity throughout the charge segregation process so that electron drift can be disregarded and the equation of electron distribution kinetics becomes a linear one. But when the electron diffusion velocity is much higher than the speed of sound (ratio of sound travel time to electron diffusion time $m >> 1$) so that absorption of light can, from the standpoint of its acoustic effect, be regarded as a superficial process involving supersonic electron diffusion within the light-absorbing skin layer. When the energy of laser action exceeds some first critical level E_2, then the electron drift velocity in a constant hole field exceeds the speed of sound and diffusion-drift balance is reached as the diffusion of excess electrons from the crystal surface into the skin layer slows down. When now also the hole drift velocity in a constant electron field is lower than the speed of sound, then the motion of holes does not significantly influence the electron distribution so that generation of sound after the transient period $t > T_{M,e}$ becomes a linear problem of piezoelectric sound generation by motion of holes. When the energy of laser action exceeds some second critical level E_3, then the hole drift velocity is higher than the speed of sound so that ambipolar diffusion of charge carriers takes place after the transient period $t > T_{M,e}$ and a quasi-neutral distribution of charge carriers is established as a result. Next is considered the case of a light-absorbing layer much thicker than the charge segregation layer, the energy of laser action having by far exceeded another critical level $E_1 > E_3$. When now the light penetration depth is much larger than the distance traveled by the sound during the charge segregation process (acoustically thick light-absorbing layer), then the sound does not have sufficient time to track changes in the electron distribution before diffusion-drift balance is established. But when the light penetration depth is much smaller than the distance traveled by the sound during the charge segregation process (acoustically thin light-absorbing layer), then the sound does have sufficient time to track changes in the electron distribution before of diffusion-drift balance is established and the intensity of the electric field set up in the process depends on the displacement of electrons by both diffusion and drift relative to stationary holes. The electron diffusion velocity is then also much lower than the speed of sound (ratio of sound travel time to electron diffusion time $m << 1$), which is however possible only as long as the energy of laser action does not exceed the critical level $E_4 = (2m)^{-1/2}E_1 > E_1$. Figures 3; references 6.

Continuous Emission Frequency Tuning of Long Pulse XeCl Laser Within 307.00-308.93 nm Band

927J0281A Moscow KVANTOVAYA ELEKTRONIKA in Russian Vol 19 No 6(240), Jun 92 pp 525-526

[Article by S. V. Yefimovskiy, A. K. Zhigalkin, Yu. I. Karev, S. V. Kurbasov, Physics Institute imeni P.N. Lebedev at Russia's Academy of Sciences, Moscow: UDC 621.373.826.038.823]

[Abstract] Failure fully to realize the potential of long pulse XeCl lasers—a promising source of ultraviolet laser radiation with an attractive pulse duration-to-efficiency (KPD) ratio—prompted a study of the outlook for expanding the XeCl laser tuning band by increasing their inversion lifetime span. To this end, a double discharge-pumped self-discharge laser with a 0.5 μs free lasing pulse duration is used; its cavity is formed by two insulator mirrors; the laser is tuned with the help of a Fabry-Perot standard (EFP) with an 11.4 focus and a 76 percent reflectance. An optical train of the experimental unit is cited and the dependence of the stimulated emission energy on the wavelength during the laser retuning with the help of the Fabry-Perot standard is plotted. The lasing spectrum is studied by a spectrograph and multichannel optical recorder on the basis of charge coupled devices (PZS). Spectral data are processed by an IBM PC/XT microcomputer. An analysis of the findings shows that the stimulated emission band can be expanded to about 1.93 nm or 202 cm^{-1} (from 307.00 to 308.93 nm) by increasing the inversion lifetime to 0.5 μs while the use of intracavity Fabry-Perot standards makes it possible to tune the long pulse XeCl laser with a 1.4 cm^{-1} line width emitting at the frequencies of the following oscillatory transitions: 0-5, 0-4, 0-3, 0-2, 0-1, 0-0, 1-7, 1-6, and 1-5. Stimulated emission by the 1-5 transition is produced for the first time. Figures 2; references 9: 2 Russian, 7 Western.

Outlook for Increasing Dual-Undulator Free-Electron Laser Gain and Efficiency

927J0281B Moscow KVANTOVAYA ELEKTRONIKA in Russian Vol 19 No 6(240), Jun 92 pp 535-538

[Article by A. V.Tulupov, Atomic Energy Institute imeni I.V. Kurchatov, Moscow; UDC 621.373.826]

[Abstract] The stimulated emission mechanism in free-electron lasers (LSE) and the relationship between the oscillation phase and particle energy are discussed and the possibility of realizing the electron bunching mechanism related to slow electron oscillations in the second undulator field of a dual undulator system is considered. This mechanism is based on a resonance with cyclotron oscillations in the longitudinal magnetic field. The electron motion in the undulator and electromagnetic wave field is examined; as a result, a free-electron laser can be developed where the base undulator is complemented with an additional undulator creating a space-periodic magnetic field in which the oscillating electrons resonate with cyclotron particle rotation in the axial magnetic field. Electron bunching may become dominant and enhance the laser gain which is inversely proportionate to the axial bunching parameter; in other words, an increase in efficiency means that the main and additional electron bunching mechanisms compensate each other. The bunching compensation mechanism may lead to autosynchronism which resembles autoresonance; this operation is possible under certain initial conditions and a fixed particle energy. References 3: 2 Russian, 1 Western.

Harmonic Generation in Dual-Undulator Free-Electron Lasers

927J0281C Moscow KVANTOVAYA ELEKTRONIKA in Russian Vol 19 No 6(240), Jun 92 pp 538-541

[Article by A. V. Tulupov, Atomic Energy Institute imeni I.V. Kurchatov, Moscow; UDC 621.373.826]

[Abstract] Heightened interest in harmonic generation in free-electron lasers is attributed to the possibility of using lower energy electron beams to stimulate emission within the same band as the fundamental frequency and make the laser smaller and cheaper. Harmonic generation in a free-electron dual-undulator laser is examined and it is noted that generally, the undulator parameter must be increased for harmonic generation. The spontaneous forward electron emission spectrum is considered and the free-electron dual undulator laser operating principle based on slow electron oscillation resonance in the additional bunching undulator's longitudinal magnetic field is explained. The formulae of harmonic generation are derived and conclusions are drawn from analyzing them. The dependence of the second and third harmonic gain on the undulator parameter is plotted. It is shown that the harmonic generation process in this free-electron laser can be controlled rather efficiently by enhancing the necessary harmonic gain and suppressing the unnecessary harmonic gain without increasing the principal undulator parameters. This is due to the fact that the longitudinal particle speed oscillates at two periods with fixed and variable amplitudes (i.e., beats). Both oscillations lead to the fundamental harmonic emission, so by selecting the conditions, one can ensure that some oscillations are dominant while others are attenuated and thus control the harmonic emission intensity. Figures 2; references 5: 2 Russian, 3 Western.

Wide-Aperture Electric Discharge Pumped Switchless XeCl Laser With 15 J Stimulated Emission Energy

927J0281D Moscow KVANTOVAYA ELEKTRONIKA in Russian Vol 19 No 6(240), Jun 92 pp 542-543

[Article by Yu. I. Bychkov, M. L. Vinnik, M. K. Makarov, High-Current Electronics Institute at the Tomsk Office of the Siberian Branch of Russia's Academy of Sciences; UDC 621.373.826.038.823]

[Abstract] The constraints imposed by the main high-current switch on the development and commercial production of electric discharge-pumped excimer lasers prompted the development of switchless designs where a preionized X-ray of ultraviolet pulse is applied after a rather slow capacitor charging; the pulse triggers a plasma-chemical processes in the active medium and stimulated emission. The results of a study of a XeCl laser with a similar pump design, an increased aperture, and higher emission pulse energy are discussed. A schematic diagram of the laser unit is cited and stimulated emission pulses at a 308 nm wavelength and a 368 and 946 nF capacitance and the dependence of the specific stimulated emission energy on the power input at a 368 and 946 nF capacitance are plotted. A 15 J stimulated pulse emission is attained at a 2.4 percent efficiency and a 4.3 active medium volume. It is noted that the laser power can be further increased by optimizing the parameters and by subsequent scaling. The absence of switches, simplicity, compactness, and good output characteristics of the design make it promising for developing a kilowatt pulse-periodic excimer laser. Figures 3; references: 2 Western.

High-Efficiency Q-Switched Er-Glass Lasers Based on Frustrated Total Internal Reflection Gate

927J0281E Moscow KVANTOVAYA ELEKTRONIKA in Russian Vol 19 No 6(240), Jun 92 pp 544-547

[Article by B. I. Denker, V. V. Osiko, S. Ye. Sverchkov, Yu. Ye. Sverchkov, A. P. Fefelov, S. I. Khomenko, General Physics Institute at Russia's Academy of Sciences. Moscow, and Moscow State Engineering University imeni N. E. Bauman; UDC 621.373.826.038.825.2]

[Abstract] Various designs of Q-spoiled Er-glass lasers—a simple and efficient source of powerful coherent radiation in the 1.5 μm spectrum band whose emission is absorbed poorly by optical glass, including quartz fibers, and the atmosphere, e.g., rotating prism, lithium niobate elecrtooptical gate, and passive gates—are discussed and attention is focused on optomechanical Q-switching gates employing the frustrated total internal reflection (NPVO) phenomenon. The parameters of such lasers which enable the designers to attain high efficiency and output energy in various operating conditions are examined. The laser cavity designs are cited and the output energy of lasers with various active media as a function of the pump energy and a typical time structure of the pulses emitted by the lasers are plotted. The optical train designs are described and the experimental procedure is outlined. An absolute flash lamp-pumped giant pulse efficiency of 0.38 percent is attained in an erbium glass laser, which is a record. The low efficiency of microsecond pulses is attributed to the nonuniform aperture filling with radiation. The findings confirm that FTIR gates are the most suitable Q-switching modulators for erbium glass lasers. Figures 3; references 11: 8 Russian, 3 Western.

All-Optical Logic Elements Based on Distributedly Coupled Optical Fibers With Nonlinear Absorption

927J0281F Moscow KVANTOVAYA ELEKTRONIKA in Russian Vol 19 No 6(240), Jun 92 pp 565-570

[Article by V. P. Torchigin, Ye. V. Sporyshev, Public Computer Center at the USSR Academy of Sciences, Moscow; UDC 621.373.826:681.3]

[Abstract] Recent trends in the development of all-optical gates and logic elements for supercomputers and

attempts to decrease the optical signal intensity by using devices in which a long-lasting interaction of short light pulses is realized during their joint propagation in nonlinear distributedly coupled optical fibers are discussed. All-optical devices developed on the basis of nonlinear distributedly coupled optical waveguides with an absorptive nonlinearity are considered. To this end, wave propagation in coupled optical waveguides with brightening media are considered and the transfer function of a CdSe single crystal, the dependence of the specific absorptance on the incident radiation intensity, the correlation of the excited wave intensity in a waveguide with absorption losses and exciting wave intensity, and the dependence of the wave intensity on the waveguide length at a weak coupling are plotted. Optical gates whose operation is based on coupled nonlinear processes and the principal characteristics and design methods of these optical elements are considered and compared to other nonresonant and resonant types of gates, e.g., Fabry-Perot resonators. For illustration, the design of a negative OR gate for two variables is shown and the condition which determines the existence of two stationary solutions of the propagation equation are derived. Figures 8; references 11: 7 Russian, 4 Western.

Emission Parameter Control of Solid-State Industrial YAG:Nd^{3+} Laser by Adaptive Optics Methods. I. Laser Cavity With Adaptive Mirror

927J0281G Moscow KVANTOVAYA ELEKTRONIKA in Russian Vol 19 No 6(240), Jun 92 pp 576-578

[Article by A. Abbas, L. N. Kaptsov, A. V. Kudryashov, T. Yu. Cherezova, Moscow State University imeni M.V. Lomonosov; UDC 621.373.826.038.825.2]

[Abstract] The urgency of controlling laser radiation parameters due to increasing uses of lasers in medicine and industry, particularly solid state lasers characterized by a relatively high efficiency and small dimensions, prompted an investigation into the possibility of developing a laser cavity for this purpose. A special program developed for computer-aided design of a laser cavity is outlined; the design is aimed at selecting the parameters of the planar and adaptive wide-aperture spherical mirrors, the meniscus, and their mutual position which ensure that the cavity is stable and the the mirror position is not critical. A schematic diagram of the cavity is cited and the dependence of the beam radius on the spherical mirror on the cavity length and the experimental dependence of the output stimulated emission power on the cavity length and pump current are plotted. The results of the experiment are consistent with theoretical data. The YAG:Nd^{3+} laser with a 5 kW pump lamp and an opaque spherical mirror is made on the basis of the design. The findings confirm the validity of the computer analysis and cavity parameter selection; the design can be successfully used for intracavity control of the spatial parameters of the output emission with the help of the adaptive spherical mirror. Figures 4; tables 3; references 4.

Emission Parameter Control of Solid-State Industrial YAG:Nd^{3+} Laser by Adaptive Optics Methods. II. Spherical Adaptive Mirror

927J0281H Moscow KVANTOVAYA ELEKTRONIKA in Russian Vol 19 No 6(240), Jun 92 pp 579-580

[Article by L. N. Kaptsov, A. V. Kudryashov, V. V. Samarkin, A. V. Seliverstov, Moscow State University imeni M. V. Lomonosov; UDC 621.373.826.038.825.2]

[Abstract] The requirement to increase the beam dimension in one of the cavity mirrors in order to use wide-aperture adaptive mirrors in solid state industrial lasers prompted the development of a laser cavity in which the collecting lens and planar controlled mirror are merged and replaced with a spherical convex mirror. An experiment where a round semipassive bimorphous concave mirror with eight control electrodes is used to control the solid state laser emission is described. The spherical bimorphous mirror design and appearance are shown and equivalent corrector response function domains are plotted. The electrode parameters are summarized. The corrector response function is measured by a modified Fizeau interferometer with subsequent interference pattern processing on a Hewlett Packard computer. The astigmatic character of surface deformation is clearly visible. The measurements show that at a power density of up to 100 W/cm^2, the corrector surface is not deformed; this confirms that the adaptive spherical mirror is suitable for intracavity control of solid state laser emission. Figures 2; tables 1; references 4.

Emission Parameter Control of Solid-State Industrial YAG:Nd^{3+} Laser by Adaptive Optics Methods. III. Decreasing Divergence and Forming Mode Structures

927J0281I Moscow KVANTOVAYA ELEKTRONIKA in Russian Vol 19 No 6(240), Jun 92 pp 581-583

[Article by A. Abbas, L. N. Kaptsov, A. V. Kudryashov, T. Yu. Cherezova, Moscow State University imeni M. V. Lomonosov; UDC 621.373.826.038.825.2]

[Abstract] Increasing uses of solid state lasers in various fields of science and engineering require sharp focusing and quick emission parameter manipulation in such lasers. An experimental unit developed for examining the possibility of controlling the mode structure and decreasing the radiation divergence of a continuous wave solid-state laser with the help of an adaptive controlled mirror inside the cavity is described and a schematic diagram of the unit is cited. The beam cross section radiation distribution in the lens focus is plotted and intensity distributions at the laser output in a unimodal operation and the mode structures in multimode lasing in the near and far fields are shown. The intracavity adaptive mirror made it possible to lower the radiation divergence by two-two and a half times in multimode lasing and obtain various shapes of mode structures (square, triangle, cross, and ring). The findings

confirm the efficacy of using intracavity adaptive mirrors for controlling the beam divergence and shaping the mode structure, which may be useful for many commercial applications. Figures 5; references 6.

On One Problem of Laser Radiation Focusing

927J0281J Moscow KVANTOVAYA ELEKTRONIKA in Russian Vol 19 No 6(240), Jun 92 pp 584-586

[Article by A. V. Goncharskiy, G. N. Morozova, O. Z. Shemkov, Moscow State University imeni M.V. Lomonosov; UDC 517.958:535.4]

[Abstract] An emerging new practical trend in laser optics—computer optics—and the issues raised by the development of computer optics elements, particularly solving the inverse problem of optical element synthesis in the framework of the selected diffraction model are discussed. An attempt is made to ascertain the suitability of the phasing optical elements designed in the ray optics approximation for focusing laser radiation into a segment with a uniform intensity distribution. The image created by the element so designed allowing for diffraction effects is studied using a more complex model where the primal problem solution is considered in Fresnel's approximation. The problem geometry is formulated analytically and graphically and the intensity distribution and background intensity distribution are plotted. An analysis of the numerical results shows that the focal segment length is not constant at different points and changes according to a certain function while the intensity distribution at the focal segment points is also not constant. The conclusion is drawn that the geometrical optics approximation in the problem of radiation focusing into a line is not consistent with the real situations, so the wave approximation should be used in subsequent analyses. Figures 6; references 3.

Physics of Two-Beam Free Electron Lasers

937J0008B Moscow VESTNIK MOSKOVSKOGO UNIVERSITETA: SERIYA 3, FIZIKA ASTRONOMIYA in Russian Vol 33 No 3, May-Jun 92 pp 64-77

[Article by V. V. Kulish, Sumy Engineering Physics Institute; UDC 537.5:621.3]

[Abstract] The issue of using the electron beam's intrinsic instability directly for generating and amplifying electromagnetic waves is addressed and attempts to accomplish this task in the past forty-plus years are discussed; the onset of free electron lasers (LSE) and relativistic electron beams (REP) renewed interest in this problem. A new type of two-beam electronic devices is outlined and the main features of the physics of two-beam free electron lasers are presented. It is suggested that the two-beam superheterodyne free electron laser technology be further developed as an alternative to today's traditional parametric lasers. The mechanisms of intrinsic two-velocity relativistic electron beam instability, quasilinear superheterodyne two-beam free electron lasers, and quadratic superheterodyne two-beam free electron lasers are considered in detail. Kinematic and amplitude wave analyses are performed. The study shows that two-beam lasers can attain a gain higher than existing analog devices by two-to-three orders of magnitude, opening up the possibility of dramatically streamlining the laser design as a whole and decreasing its weight, overall dimensions, and cost. The conclusion is drawn that in the area of low and medium power, two-beam free electron lasers may become the principal amplification systems in the submillimeter and infrared bands. Figures 4; tables 2; references 22: 20 Russian, 2 Western.

Characteristics of Spectral Dependence of External Radiation Gain in Semiconductor Laser

927J0278C St. Petersburg PISMA V ZHURNAL TEKHNICHESKOY FIZIKI in Russian Vol 18 No 9, May 92 pp 20-22

[Article by K. B. Dedushenko, M. V. Zverkov, V. P. Konyayev, A. N. Mamayev; UDC 06.3; 07]

[Abstract] It is speculated that laser amplifiers will gain increasing uses in future optical communication systems, making it necessary to examine their characteristics in detail. The spectral dependence of the laser gain with a weak radiation injection is observed at the moment before the mode locking, i.e., when the laser is still used as a tuned amplifier. To this end, radiation from a PL1 semiconductor injection laser which serves as an external radiation source is injected into a PL2 semiconductor laser which serves as an amplifier. Faraday's isolation is used to prevent the spurious effect of the PL2 laser. An optical train of the experimental unit is cited and the dependence of the output power on the injected radiation frequency at the lasing action threshold and 20 percent above the threshold are plotted. At the threshold or 5-10 percent above it, a conventional dependence of the laser gain on frequency, peaking at the coincidence of the external radiation frequency with the laser's natural resonance frequency, is observed. Yet when the threshold is exceeded by 10-20 percent or more, the injected radiation power remains so low that locking does not occur and a fine structure in the form of proximate maxima appears in the amplification circuit whereby the maxima are equidistant at a low injected luminous power. It is speculated that the findings can be attributed to the nonlinear interaction of external radiation with the laser mode field. Figures 2; references 5: 1 Russian, 4 Western.

Role of Particles of Target Material in Dynamics of Laser Erosion Flare

927J0265A Minsk INZHENERNO-FIZICHESKIY ZHURNAL in Russian Vol 65 No 5, May 92 (manuscript received 12 Nov 91) pp 665-684

[Article by V. K. Goncharov, Scientific Research Institute of Applied Problems in Physics imeni A. N. Sevchenko, Minsk; UDC 621.373.826:533.9]

[Abstract] The action of medium-intensity laser radiation (0.1-100 MW/cm^2 on metals during their treatment is examined on the basis of experimental data and theory, considering that the incident laser radiation interacts not only with the target surface but also with the erosion products and those in turn can prevent at least some further radiation from reaching that surface. In an experiment concerning this problem (V.K. Goncharov, V.I. Karaban, A.V. Kolesnik; KVANTOVAYA ELEKTRONIKA Vol 12, 1985) the erosion flare of such a medium-intensity neodymium laser was probed with a low-intensity ruby laser by measuring the radiation energy balance of the latter along its path. Radiation pulses of up to 1.5 kJ total energy and 1 ms duration from the neodymium laser operating in the free emission mode were focused through a lens with focal length of 25 cm within a spot 7.5 mm in diameter on the surface of a zinc target, the incident laser power being varied by means of neutral glass filters. The ruby laser emitted regular radiation spikes in trains of 1.5 ms total duration, its beam designed to probe the erosion flare at a distance of 1.5 mm above the target surface and its diameter being varied over the 1.5-2.0 mm range. The intensity of the ruby laser radiation was 10 kW/cm^2, sufficiently low as not to perturb the eroded medium. The energy characteristics of both lasers were measured with IKT-1N calorimeters. Each laser was aligned by means of an He-Ne laser. The ruby laser beam was passed through a beam splitter plate directly, the neodymium laser beam first through two successive amplifier stages. The time characteristics of neodymium laser radiation were monitored by an FD-9 photodiode. Three other FD-9 photodiodes measured the power of ruby laser radiation prior to incidence on the erosion flare, transmitted by the erosion flare, and scattered by the erosion flare respectively. Interference filters tuned to the ruby laser wavelength were placed one before the photodiode monitoring the neodymium laser radiation and one before the photodiode measuring the ruby laser radiation transmitted by the erosion flare, so as to eliminate any interference from those two radiation sources (neodymium laser and erosion flare) on the readings of ruby radiation energy transmitted and scattered by the erosion flare. Both electron temperature and electron concentration in the flare plasma were measured with the aid of a spectrometer and a high-speed streak camera. The data are processed and interpreted in accordance with various applicable theories, scattering of ruby laser radiation by zinc particles liquefied into droplets being the most probable mechanism explaining the kinetics of its transmission and absorption as well as scattering (both Rayleigh scattering and Thompson scattering are ruled out). This scattering mechanism is then analyzed further by involving the particle size factor, the two extreme cases being particles much smaller and much larger than the wavelength of probing radiation. The theory is extended to particles of metals other than zinc such as pure copper and molybdenum alloys of copper. With respect to their behavior and specifically their erosion under laser treatment, all metals studied in this and other experiments fall are tentatively classified on the basis of their boiling point: 1) those with a low boiling point (Cd, Pb, Zn, Bi, Mg); 2) those with an intermediate boiling point (Al, Cu, Ni); 3) those with a high boiling point (Ti, Mo, W). As the intensity of laser action on a metal target increases, bulk vaporization of the latter generates an increasing amount of particles which enter the erosion flare originally consisting of transparent vapor, where they scatter and absorb incident laser radiation. Then moving against the incident laser beam, they evaporate completely and generate a surrounding medium denser than one generated by adiabatic expansion of that original transparent particles and, as the laser radiation intensity reaches some critical level different for each metal, some of them initiate plasma flashes in their vicinity. The number of these flashes increases until the particles have almost completely evaporated. The theoretical plasma-breakdown laser radiation intensity lies within: 0.25- 2.15 MW/cm^2 for Bi, 0.3-0.9 MW/cm^2 for Pb, 0.7- 1.1 MW/cm^2 for Ti, 0.7-1.9 MW/cm^2 for Cd, 0.7- 2.2 MW/cm^2 for Mg, 0.9-2.65 MW/cm^2 for Zn; 1.3-3.0 MW/cm^2 for Al; 1.6-3.3 MW/cm^2 for Ni, 1.7-4.8 MW/cm^2 for Mo, 2.6-4.2 MW/cm^2 for W, 4.0- 12.0 MW/cm^2 for Cu. Figures 14; references 44.

Recrystallization of Thin GaAs Films on Si by Pulsed Laser Treatment

927J0267A Minsk IZVESTIYA AKADEMII NAUK BYELARUSI: SERIYA FIZIKO-MATEMATICHESKIKH NAUK in Russian No 2, Mar-Apr 92 (manuscript received 8 Oct 90) pp 41-44

[Article by G. D. Ivlev and F. M. Katsapov, Institute of Electronics at Byelarusian Academy of Sciences; UDC 621.315.592]

[Abstract] In an experiment thin (less than 1 μm thick GaAs films) were grown on Si(100) substrates by MOS-hydride epitaxy, some with and others without prior chemical treatment of the substrates for removal of the oxide surface layer, and then treated with radiation from a monopulse ruby laser in pulses of about 70 ns duration. The energy delivered by these pulses was varied over the 0.2-1.4 J/cm^2 range, the energy carried by successive pulses deviating not more +/-5 percent from the fixed nominal level and the energy density being distributed uniformly within +/-(5-10) percent over target spots 3-6 mm in diameter. Structural examination of the films was performed under a scanning electron microscope, in an electron diffractometer, in a mass spectrograph, and by X-ray photoelectron spectroscopy. In their initial state the GaAs films appeared in either polycrystalline or single crystal form. The polycrystalline ones grown without chemical pretreatment of the substrates were found to recrystallize again into a polycrystalline form when the oxide interlayer was about 2 nm thick SiO_2, such an interlayer having breached the conditions for heteroepitaxial growth of GaAs from the melt, or to recrystallize into a single crystal form when that interlayer was not thicker than about 1 nm. The films grown on chemically pretreated substrates into a single crystal

form were found to recrystallize by liquid-phase epitaxy into a single crystal form again. Melting of polycrystalline GaAs films by pulsed heating was found to make to surface after recrystallization smoother, more effectively so when the energy density of incident radiation had been increased from 0.5-0.8 J/cm^2, and to make it rougher owing to ejection of some of the film material without impairment of the substrate surface when the energy density of incident radiation had been raised to 1.2 J/cm^2. Figures 1; references 6.

Laser-Stimulated Desorption of Charged Particles in Weak Electric Fields

927J0267B Minsk IZVESTIYA AKADEMII NAUK BYELARUSI: SERIYA FIZIKO- MATEMATICHESKIKH NAUK in Russian No 2, Mar-Apr 92 (manuscript received 12 Sep 90) pp 65-71

[Article by V. P. Volkov, P. A. Skiba, and A. G. Sechko (deceased), Mogilev Department, Institute of Physics imeni B. I. Stepanov at Byelarusian Academy of Sciences; UDC 621.373.8:535.51]

[Abstract] An experimental study concerning desorption of charged particles from a surface treated with radiation from a pulsed ruby laser in a weak electric field (E > 15 kV/cm) was made, of interest being the dependence of the desorbed ion flux on both electric field and laser radiation intensities. The surface of ferrite and glass-ceramic specimens was irradiated inside a vacuum chamber under a residual pressure of 1.3 Pa while an electric potential was being applied to a ring electrode about 5 mm above that surface. The ruby laser, inside a spherical optical cavity ensuring its regular mode of operation, delivered rectangular radiation pulses of 600 μs duration to 7 mm^2 large surface spot, their energy being varied up to 3 J maximum with the energy carried by successive pulses in each test deviating not more than +/-5 percent from the nominal level. The electric potential at the electrode was varied over the 0-150 V range, a fresh specimen being tested at each voltage level. The desorbed ions were collected by a hollow metal cylinder grounded through a resistor and the voltage drop across this resistor, produced by neutralization of charges on that collector surface, was recorded with an oscillograph. The parameters of ion current pulses generated during laser treatment at a constant energy level were found to depend on the polarity of the applied potential and on the number of successively incident radiation pulses, noteworthy being the nonmononotonic dependence of the ion current density j around the grounded collector on the applied voltage V. That ion current density, characterizing the rate of their desorption, was also found to depend nonmonotonically - though more mildly so - on the density F of incident laser pulse energy. The results of this study are interpreted by considering in their analysis collisions of free ions and molecules above the adsorbent surface in an external electric field. In a weak electric field this process can be regarded as one consisting of two stages: thermal desorption of neutral molecules followed by their ionization near the surface. Calculations for positive ions desorbed from a metal plate at ground potential are made on the basis of 1) the Yegorov-Letokhov-Shibanov relation (KVANTOVAYA ELEKTRONIKA, Vol 11 No 7, 1984) for the rate of decrease of the surface density of adsorbent particles $dn/dt = -n\nu \exp[(-\varphi/kT(t)]$ (ν- characteristic vibration frequency of adsorbate molecules, φ- desorption activation energy, T- surface temperature, k=- Boltzmann constant), where the surface temperature is a function of time according to the Ready relation $T = 2(1-R)F(at/\pi)^{1/2}/k$ (R- reflection coefficient at target surface, F- density of incident radiation energy, a- thermal diffusivity of adsorbent material, k- thermal conductivity of adsorbent material) and 2) the Langmuir-Saha equation for the ratio of charged particle to neutral particle fluxes. The results indicate that even a weak external electric field near the adsorbent surface can strongly influence the magnitude of the ion flux density attainable during pulsed laser treatment of that surface. This ion current density j passes through successively higher maxima both when the voltage V is raised while the radiation energy density is held constant and when the radiation energy density F is raised increased while the voltage V is held constant, the magnitudes of V at F= const and of F at U= const as well the magnitudes of these current density maxima depending on the initial adsorbate density, the desorption process parameters, and the probability of inelastic ion-molecule collisions. Figures 3; references 9.

New Low-Threshold $LiKYF_5:Nd^{3+}$ Laser Crystal

927J0269A Moscow KVANTOVAYA ELEKTRONIKA in Russian Vol 19 No 3(237), Mar 92 pp 213-215

[Article by A. A. Kaminskiy, N. M. Khaydukov, Crystallography Institute imeni A. V. Shubnikov at the USSR Academy of Sciences, Moscow, and General and Inorganic Chemistry Institute imeni N. S. Kurnakov at the USSR Academy of Sciences, Moscow; UDC 621.373.826.038.825.2]

[Abstract] The failure of many anisotropic fluorides with an ordered structure activated by Nd^{3+} ions to ensure sufficient optical quality of laser fluoride crystals at the necessary Nd^{3+} ion concentration, primarily due to the poor physical and chemical characteristics of these compounds, prompted a search for new single-center low-threshold fluorides with Nd^{3+} ions for diode-pumped crystal lasers. A newly discovered $LiKYF_5:Nd^{3+}$ laser fluoride crystal is described, its low-threshold stimulated pulse emission (SI) is examined, and the crystallization conditions are determined. A concentrational series of crystals is grown by the hydrothermal method, resulting in samples with up to 3 mm in diameter; 2 mm thick active elements are subsequently made from these crystals. The 300 and 77K luminescence spectra and the spectrum splitting diagram of the new crystal are plotted. Pulsed emission is stimulated by the transitions of the principal lasing channel. It is speculated that the new laser crystal will be more attractive for diode-pumped

lasers than available fluoride crystals. Figures 2; tables 1; references 6: 2 Russian, 4 Western.

Controlling XeCl Laser Radiation Divergence in Amplification Mode

927J0269B Moscow KVANTOVAYA ELEKTRONIKA in Russian Vol 19 No 3(237), Mar 92 pp 219-221

[Article by S. Ye. Kovalenko, V. F. Losev, High-Current Electronics Institute, Tomsk; UDC 621.373.826.038.823]

[Abstract] The need to attain a high radiation luminosity in excimer lasers which calls for using multistage circuits where the amplifier is used in the single- and double-pass mode and injection locking (IS) and the lack of comparative studies of these conditions prompted an examination of the output characteristics of an electric-discharge XeCl laser in the single-pass and injection locking modes. An optical train of the experimental unit is cited and the behavior of the energy fraction contained within a 48 μrad angle under amplification and within an 88 μrad angle under injection locking, the output energy behavior under amplification and relative energy increment under injection locking as a function of the delay tine, and the angular emission energy distribution of the master oscillator (ZG) for single-pass amplification, injection locking, and free lasing with an unstable resonator are plotted. The laser radiation divergence is assessed using a lens and by the energy of the beam transmitted through a calibrating orifice. Spectral measurements are taken by an IT-28-30 interferometer. The narrow-band radiation divergence after a single-pass amplification is virtually the same along and across the electric field; the radiation energy in the injection locking mode is more than twice that of the single-pass amplification mode (or 90 vs. 35 mJ). Under typical energy parameters of the master oscillator with a 400 W power, the highest radiation luminance is attained in an amplifier with a pumping duration of several tens of nanoseconds in the injection locking mode. Figures 3; references 6: 4 Russian, 2 Western.

Stimulated Emission of Collective Modes in Two Optically Coupled CO_2 Lasers

927J0269C Moscow KVANTOVAYA ELEKTRONIKA in Russian Vol 19 No 3(237), Mar 92 pp 224-230

[Article by V. V. Antyukhov, Ye. V. Danshchikov, I. V. Masyukov, Atomic Energy Institute imeni I. V. Kurchatov, Moscow; UDC 621.373.826.038.823]

[Abstract] The possibility of using coupled lasers for increasing the radiation luminance exponentially while maintaining a good radiation quality (in coherent operation) prompted an experimental investigation and a numerical analysis of the stimulated emission of collective modes in two optically coupled CO_2 lasers. A mathematical model is developed for numerical studies in a planar wave approximation and single- and two-mode lasing conditions and lasing stability are examined. An optical train of the experimental unit is cited and the dependence of the lasing frequency and beats on the frequency detuning, the dependence of the output laser power on detuning, the relationship of the effective phase and phase difference between the output beams of individual collective modes, the dependence of the luminous intensity and interference band peak intensity on detuning, and the dependence of the interference band luminosity on detuning are plotted. An analysis shows that a partial luminosity gain can be realized from two lasers by rather crude resonator length tuning system without holding it within the lock band due to the interference patterns in the multifrequency lasing condition. The advantages of coupled lasers are especially evident in the case of phased lasing but it is necessary to maintain the resonator length near the zero detuning. The phase incursion must be carefully controlled in the channel in order to maximize the gain and ensure equal and maximum laser output intensities. Figures 7; references 8: 5 Russian, 3 Western.

New Semiconductor Laser Radiation-Pumped Crystal Lasers Based on Disordered Fluorides Doped With Nd^{3+} Ions

927J0282A Moscow KVANTOVAYA ELEKTRONIKA in Russian Vol 19 No 2(236), Feb 92 pp 109-111

[Article by A. A. Kaminskiy, H. R. Verdun, Crystallography Institute imeni A. V. Shubnikov at the USSR Academy of Sciences, Moscow, and Fibertek Inc., Herndon, VA, USA; UDC 621.373.826.038.825.2]

[Abstract] Continuous wave single-mode stimulated emission (SI) of the Nd^{3+} activator dopant excited by the radiation of a GaAlAs laser diode array at a 300K temperature is reported in nonstoichiometric disordered fluoride-based crystal lasers (Ca-Y, Sr-Gd, Ba-Y, and Ba-La fluorides with a *Fm3m* fluorite structure). Single crystals of the multicomponent fluoride systems with a heterovalent isomorphism where fluorine atoms occupy new positions which differ from 1/4, 1/4, and ¼ are grown by the Bridgeman and Stockbarger method. The lasing characteristics of the disordered fluoride crystals doped with Nd^{3+} ions at 300K are summarized and the active absorption spectra fragments of the Nd^{3+} ions in disordered fluorite-structured crystals at 300K are plotted. The optical train of the laser and the anamorphic optical prism system is shown. The principal element of the laser is a 1 W SDL-2460-C diode laser array developed by the Spectra Diode Laboratories. The experiment confirms the possibility of stimulating a CW single-mode emission of the Nd^{3+} ions at room temperature in the $^4F_{3/2} \rightarrow {}^4I_{11/12}$ lasing channel in disordered fluorite-type fluoride crystals. It is speculated that the lasing parameters will be improved and emission will be stimulated by other intermultiplet transitions. The authors are grateful to V. Koeschner and Ti Chuang for assistance and support. Figures 2; tables 1; references 10: 3 Russian, 7 Western.

New Disordered $Ca_2Ga_2SiO_7:Nd^{3+}$ Crystal for High-Power Solid State Lasers

927J0282B Moscow KVANTOVAYA ELEKTRONIKA in Russian Vol 19 No 2(236), Feb 92 pp 111-113

[Article by A. A. Kaminskiy, V. A. Karasev, V. D. Dubrov, V. P. Yakunin, B. V. Mill, A. V. Butashin, Crystallography Institute imeni A. V. Shubnikov at the USSR Academy of Sciences, Scientific Research Center of Industrial Lasers at the USSR Academy of Sciences, Shatura, Moscow oblast, and Moscow State University imeni M. V. Lomonosov; UDC 621.373.826.038.825.2]

[Abstract] Analogues of helenite and akermanite minerals are discussed due the possibility of growing single crystals and using them in modern optics and quantum electronics devices, especially when doped with Nd^{3+} ions. Thus, Nd^{3+}-doped Ga-helenite which is promising for use in conventionally lamp-pumped high-power pulsed lasers is considered; to this end, rather large single crystals are grown with the optimum activator ion concentration and subjected to lasing-energy tests. The Nd^{3+} ion luminescence spectra in $Ca_2Ga_2SiO_7:Nd^{3+}$ crystals and the dependence of the lasing energy on the pumping energy at 300K are plotted and the spectral-lasing characteristics of the Ca-helenite crystals doped with Nd^{3+} ions are summarized. A K-301 quantron with an EDNP-6/90 Xe pulse lamp is used as the illuminating system. The lasing line width is greater at cryogenic temperatures than at room temperature while the type of absorption and luminescence spectra changes little with temperature, which is typical of disordered laser media. In the principal lasing channel, an output energy of 4 J is attained at a total efficiency of 1.7 percent in the pulsed mode; in the pulsed periodic mode at a 10 Hz frequency, the laser efficiency is 1.5 percent. The refractive indices of the crystals in the $^4F_{3/2} \rightarrow {}^4I_{11/12}$ lasing channel are 1.7132 and 1.7029. The experiment demonstrates that disordered $Ca_2Ga_2SiO_7:Nd^{3+}$ crystals are suitable for developing high-power solid state lasers. Figures 2; tables 1; references 12: 2 Russian, 10 Western.

Injection Locking in High Power XeCl Laser

927J0282C Moscow KVANTOVAYA ELEKTRONIKA in Russian Vol 19 No 2(236), Feb 92 pp 133-134

[Article by Yu. I. Bychkov, N. G. Ivanov, S. Ye. Kovalenko, V. F. Losev, Yu. N. Panchenko, High Current Electronics Institute at the Siberian Department of the USSR Academy of Sciences, Tomsk; UDC 621.373.826.038.823]

[Abstract] The use of injection locking (RIS) for improving the quality of high-power excimer laser radiation is discussed and the lack of consistent published data on the subject matter is noted. An experiment with an XeCl laser excited by two electron counterbeams is described and the optical train of the experimental unit is cited. The injected radiation is generated by a system of two electric discharge lasers with injection locking; the output radiation energy is 100 mJ at a 100 ns pulse duration. Oscillograms of the output and injected pulses emitted by the 0-1 and 0-2 transitions at various lasing pulse delays relative to the external pulse and the radiation spectrum density curves in the free lasing operation and with 0-1 line injection are cited. The study of the injection-locked operation in an XeCl laser with a 300 ns pulse shows that up to 90 percent of the energy can be concentrated in the injected line provided that the cavity's axial area is filled with the external signal exceeding the spontaneous noise level from the start of pumping to the lasing action threshold while the spectrum control efficiency worsens upon reaching the trailing edge. Compared to free lasing, radiation divergence improves slightly in injection-locked operation. Figures 3; references 6: 1 Russian, 5 Western.

Iodine Laser Pumped by Shock Wave Front Light Created by Explosive Charge Detonation

927J0282D Moscow KVANTOVAYA ELEKTRONIKA in Russian Vol 19 No 2(236), Feb 92 pp 135-138

[Article by V. P. Arzhanov, B. L. Borodich, V. S. Zuyev, V. M. Kazanskiy, V. A. Katulin, G. A. Kirillov, S. B. Kormer (deceased), Yu. V. Kuratov, A. I. Kuryapin, O. Yu. Nosach, M. V. Sinitsyn, Yu. Yu. Stoylov, All-Union Scientific Research Institute of Experimental Physics, Arzamas, and Physics Institute imeni P.N. Lebedev at the USSR Academy of Sciences, Moscow; UDC 621.373.826.038.823]

[Abstract] The outcome of numerous studies carried out since the onset of lasers in the early 60's, and especially in 1965-1966 while examining the possibility of developing high-power lasers, are summarized. The efforts in question were aimed at increasing the pump power and using large active medium volumes. Attention is focused on the development of photodissociation lasers whereby the lasing effect is attained during the photodissociation of a certain class of chemical compounds, e.g., gaseous trifluormethane, and lasing is achieved by transitions in the near infrared spectrum at 1.316 μm. The experiment design is formulated and the experimental findings are discussed; the dependence of the radiation energy on the CF_3I pressure, the dependence of lasing boundary speed on the pressure, and the angular energy distribution are plotted. In the experiment, the laser is pumped by the light generated by the shock wave front of an explosion whereby the working medium is excited by the shock wave in Xe and in a mixture of the working medium with an inert gas. In the latter case, the energy characteristics are much higher: the laser pulse energy reaches 100 J at a 15 MW mean power. Laser radiation divergence is measured, showing that at a half-power level, the beam diverges by close to 4 μrad which exceeds the limit of diffraction by almost two orders of magnitude, probably due to active medium inhomogeneities. Figures 7; tables 2; references 6: 5 Russian, 1 Western.

Optically Pumped Submillimeter CD_3COND_2 and ND_2CD_2COOD Molecule Lasers

927J0282E Moscow KVANTOVAYA ELEKTRONIKA in Russian Vol 19 No 2(236), Feb 92 pp 139-140

[Article by L. D. Fesenko. A. Ya. Ovcharenko, Kharkov Engineering Teachers Institute imeni I. Z. Sokolov; UDC 621.373.826.038.823]

[Abstract] The advantages of optically pumped submillimeter wave lasers (SM) both in basic and applied research prompted a search for new active media for such lasers. CW stimulated emission of CD_3COND_2 and ND_2CD_2COOD molecules (acetamide-D_5 and glycine-D_5, respectively) in the submillimeter band pumped by the radiation of a CO_2 laser is reported and the experimental unit used for this purpose is described. The 20 W pump laser is tunable within a 9.2-10.8 μm band while the submillimeter band radiation is detected by a high-speed point contact detector with an InSb-beryllium bronze pair and a pyroelectric detector at room temperature. The lasing characteristics and radiation polarization are summarized. The experiment resulted in generating nine lasing lines within the 303-545 μm band and five lines within the 86-973 μm band. A continuous wave radiation power of up to 150-200 mW can be attained which is sufficient for most practical applications. Tables 1; references 2.

Active Mode-Locked Picosecond Cr-Yb-Er Glass Laser

927J0282F Moscow KVANTOVAYA ELEKTRONIKA in Russian Vol 19 No 2(236), Feb 92 pp 140-142

[Article by A. B. Grudinin, Ye. M. Dianov, B. I. Denker, V. G. Kozlov, S. Ye. Sverchkov, A. K. Senatorov, General Physics Institute at the USSR Academy of Sciences, Moscow; UDC 621.373.826.038.825.3]

[Abstract] Active mode-locking (ASM) in solid state lasers—an efficient means of generating laser pulses with a picosecond duration—and the principal advantages of this method, i.e., the high stability and reproducibility of the resulting laser pulses prompted analyses of ASM method; as a result, a formula is derived for the steady-state pulse duration in a laser with a uniformly broadened line. An experiment with a pulsed laser with a phosphate Cr-Yb-Re glass is conducted and the experimental unit's layout is shown. The time characteristics of the laser are examined and an oscillogram of the laser pulse fragment and a typical pulse shape produced by digital image processing from the image converter screen are plotted. A $LiNbO_3$ crystal high-efficiency modulator made it possible to generate 13+/-5 ps pulses at a 1.54 μm wavelength with a 100 kW peak power in the active mode-locking operation. This wavelength is selected because it falls within the minimum quartz fiber loss range. Figures 3; references 5: 1 Russian, 4 Western.

Efficient LiF Crystal (F_2) Tunable Lasers With F_2^- and F_2^+ Color Centers

927J0282G Moscow KVANTOVAYA ELEKTRONIKA in Russian Vol 19 No 2(236), Feb 92 pp 145

[Article by T. T. Basiyev, V. A. Konyushkin, S. B. Mirov, V. V. Ter-Mikirtychev, General Physics Institute at the USSR Academy of Sciences, Moscow; UDC 621.373.826.038.825]

[Abstract] The task of developing highly efficient color center (TsO) lasers with a continuously tunable lasing line and elevated efficiency (KPD) and active element (AE) service life is accomplished by optimizing the laser fabrication practices. The high quality of the LiF crystal active media (by the $F_2 \rightarrow F_2^+$ transitions) is confirmed by the lasing parameters obtained in a nonselective cavity. An optical train of the wide-band tunable pulse-periodic laser is cited and the service life diagram (i.e., the radiating power) of the LiF active medium with a single pump channel is plotted. The laser is pumped by the second harmonic of a YAG:Nd^{3+} laser emitting at a 0.532 μm wavelength. The incident energy efficiency of the optimized laser is 38 percent and the absorbed energy efficiency—41 percent; the former figure can be increased to 47 percent using an irradiated cooled LiF crystal. Wide-band lasing life reaches 15 min at an incident radiation density of 40 MW/cm^2 at a repetition frequency of 12.5 Hz; the active medium remains serviceable for almost ten hours. Figures 2; references 3.

Parameter Optimization of Dynamically Stable CW-Pumped Solid-State Laser Cavities

927J0282H Moscow KVANTOVAYA ELEKTRONIKA in Russian Vol 19 No 2(236), Feb 92 pp 175-179

[Article by M. I. Demchuk, I. A. Manichev, V. P. Mikhaylov, G. A. Pribytok, A. K. Khoroshun, Scientific Research Institute of Applied Physical Problems imeni A. N. Sevchenko at the Belarussian State University imeni V. I. Lenin, Minsk; UDC 621.373.826.038.825]

[Abstract] The task of maximizing the TEM_{00} mode volume is examined theoretically and experimentally and the stability zone width of dynamically stable cavities is analyzed in order to determine the cavity parameter ranges within which the effect of the laser system instability sources can be minimized. The study is prompted by the increasing use of solid state CW pumped lasers in CW, Q-spoiling, mode-locking, and intracavity harmonic generation operations and their combinations. A cavity is analyzed numerically using a mathematical model based on Magni's simplified routine; the experimental unit design is cited and the formulae which characterize the internal lens cavity parameters are derived. All computations are made using nondimensional quantities, making it possible to apply the results to all types of cavities. The maximum mode radius in the active element in the middle of the stability zone, the stability parameter, experimentally measured focal lengths of the induced thermal lens

(NTL) in the YAG:Nd^{3+} crystal for the sagittal and tangential components, and the dependence of the active element mode radius on the focal length of the internal thermal lens and the distance from the mirror are plotted. The pump and stimulated emission intensity as a function of time and spectral pump and stimulated emission intensity distributions are examined. The findings show that the cavities in which the stability zone greatly exceeds the width of the induced thermal lens astigmatism ensure a spatially uniform Gaussian radiation profile at the output and in the far-field zone and a minimal emission instability level which does not exceed the pump instability. Figures 7; tables 1; references 14: 3 Russian, 11 Western.

Bimorphous Adaptive Mirror

927J0282I Moscow KVANTOVAYA ELEKTRONIKA in Russian Vol 19 No 2(236), Feb 92 pp 180-183

[Article by A. V. Ikramov, S. V. Romanov, I. M. Roshchupkin, A. G. Safronov, A. O. Sulimov, Kompozit Scientific Production Association, Kaliningrad, Moscow oblast; UDC 681.7.062.47]

[Abstract] The use of mirrors with a controllable reflecting surface for improving the characteristics of today's optical systems and expanding their capabilities and the advantages of bimorphous adaptive mirrors for this purpose are discussed. A copper cooled bimorphous adaptive mirror developed on the basis of a double bimorphous structure and intended for equalizing the large-scale optical aberrations, including those in up to 15 kW systems, is considered. The design of the adaptive mirror and its components is described and its schematic diagram is cited. The adaptive mirror has 19 electrodes which include two piezoelectric plates and ring sectors. The normative response functions of the control electrode in the lower piezoelectric plate of the external and middle rings and the low-order aberration approximation of the adaptive mirror are plotted. The piezoelectric ceramic electrode are made from the TsTS-19 and TsTSNV-1 ceramics; the maximum control voltage is +/-300 V. Interferometry analyses are performed by a Mark-III interferometer made by Zigo and the response function is plotted by an interferometer with subsequent computer processing. The findings show that the adaptive bimorphous mirror is capable of operating efficiently in optical systems as a low-order aberration compensator due to the high reflecting surface deformations while the mirror's frequency response make it suitable for use in systems with a frequency spectrum of up to 2 kHz. Figures 6; references 6: 4 Russian, 2 Western.

Emission of Charged Particles During Slow Negative Pion Capture by Uranium Nuclei

937J0018A Moscow YADERNAYA FIZIKA in Russian Vol 55 No 9, Sep 92 pp 2319-2324

[Article by G. Ye. Belovitskiy, V. N. Baranov, C. Petitjean, Nuclear Research Institute at Russia's Academy of Sciences and Paul Scherrer Institute, Switzerland]

[Abstract] The effect of π^--mesons captured by heavy nuclei on the emission of Auger electrons and X-rays and the resulting transitions to mesoatomic states are discussed and the fission of uranium nuclei by slow negative pions accompanied by emission of charged *p, d, t,* and α-particles is examined. To this end, the angular and energy distributions and the emission probability of charged particles accompanying the uranium nuclei fission by slow pions are investigated. The angular distributions are measured in relation to the heavy fragment movement direction. Nuclear 150-μm-thick photoemulsions manufactured at the NII of Chemical and Photo Design are used as the target and charged particle detector for recording protons with an up to 150 MeV energy. The emulsions are irradiated in a πE1 beam at the Paul Scherrer Institute in Switzerland at a 100 MeV/*c* momentum. The energy and angular distributions of α-particles are plotted and the emission mechanism of heavy fragments is discussed. A twofold discrepancy between the experimental results and theoretical data for the number of particles emitted in, and against, the fragment movement directions is noted. The effect becomes more pronounced with an increase in the fission asymmetry and with a decrease in the particle energy. The observed anisotropy is attributed to the fact that the particles are predominantly emitted by heavy fragments and nonisotropically. In addition, the existence of another mechanism favoring the charged particle emission in the heavy fragment motion direction is suggested. The need to study the dependence of the above phenomenon on the energy and type of the primary particle and the target nucleus mass is noted. Figures 4; tables 1; references 15: 7 Russian, 8 Western.

Investigation of Extraordinary ^{238}U Neutron Resonances

937J0018B Moscow YADERNAYA FIZIKA in Russian Vol 55 No 9, Sep 92 pp 2325-2332

[Article by M. A. Voskanyan, G. V. Mozolev, G. V. Muradyan, V. A. Stepanov, L. P. Yastrebova, Kurchatov Institute, Moscow]

[Abstract] Observations of two ^{238}U neutron resonances at a 721.58 and 1,211.4 eV energy distinguished by abnormally large fission widths which are usually explained in the framework of the model of a double-hump fission barrier are reported and such ^{238}U neutron resonances are examined from two aspects: by measuring scattering in order to establish the radiation width of the 721 and 1,211 eV resonances independently and answer the question of whether they have an additional fission channel and by studying the γ-cascades. The measurement procedure is outlined and it is noted that a high relative aperture technique is necessary to measure scattering. The design of a multisection 4π-detector which makes it possible to identify scattering events is described and the dependence of the number of scattering events on the time-of-flight channel number in the resonance region and the ratio of the 290.94, 1,211.4, 721.58 eV resonance areas to the 397.59 eV resonance area as a function of the coincidence ratio based on the measurement results with a thick sample are plotted. An analysis shows that if there are no additional channel in the 721 eV resonance with an 8 meV width (which is unlikely) and it is due to an extraordinary state, the intrinsic width of this state is much less than 3.2 meV. This extraordinary state is not the second well state from the double-hump fission barrier model since its width is 4 meV. The extraordinary state is noteworthy in that is it characterized by a high 4.8 MeV energy and a low ½ spin. Figures 3; tables 1; references 14: 4 Russian, 10 Western.

Fragment Properties and Prompt Uranium Fission Neutron Emission

937J0018C Moscow YADERNAYA FIZIKA in Russian Vol 55 No 9, Sep 92 pp 2333-2339

[Article by A. A. Goverdovskiy, V. A. Khryachkov, V. F. Mitrofanov, N. N. Semenova, Energy Physics Institute, Obninsk]

[Abstract] Fission of uranium nuclei into two fragments with a total kinetic energy close to the reaction energy is considered and it is noted that away from the fission barrier apex, prompt neutron emission becomes allowed from the energy viewpoint both from separated fragments and from the fission system itself during the post-saddlepoint movement toward the rupture whereby both emission processes are on a different scale and contribute different types of distortions to the fragment properties observed. An attempt is made to examine the fragment properties and identify and assess these two emission processes. The fission fragment spectrometry method is outlined and the mass vs. energy fragment spectra of ^{238}U fission by thermal neutrons are examined. The fragment yield contours of ^{238}U fission by thermal neutrons, a graphic description of the fragment spectrum by Gaussian curves, data on the mean yields of prompt fission neutrons from fragments, and the shift of the mass components centers of the fragment spectra as a function of the light fragment energy are plotted. An analysis of the mass vs. energy fragment spectra of low-energy uranium fission confirms the likelihood that multiple neutron emission exists prior to the nucleus fission into fragments but after passing the fission barrier's saddlepoint. The prefission neutron emission is most likely at the early post-saddle evolution stage of the system and makes therefore an extremely small contribution to the integral prompt neutron yield (MND). It is speculated that direct experimental observations of the

angular neutron vs. fragment correlations at high kinetic fragment energies are promising. The prefission component contribution is estimated to be on the order of 10^{-3}. Figures 4; references 22: 6 Russian, 16 Western.

Neutron Emission Spectra of ^{239}Pu Nuclei

937J0003A Moscow YADERNAYA FIZIKA in Russian Vol 55 No 8, Aug 92 pp 2017-2023

[Article by G. N. Lovchikova, A. V. Polyakov, S. E. Sukhikh, A. M. Trufanov, Energy Physics Institute, Obninsk]

[Abstract] The lack of experimental data on the fast neutron interaction with ^{239}Pu nuclei and other fissionable isotopes necessary both for practical nuclear power plant design tasks and for theoretical studies prompted an investigation into the secondary neutron spectra produced under an interaction of neutrons at a 4,92 and 5.74 MeV initial energy with fissionable 239Pu nuclei. The measurements are taken in a time-of-flight neutron spectrometer in a cylindrical geometry; to this end, detector designed on the basis of a stilbene crystal and a FEU-30 photomultiplier is used. The experiment is conducted in an EGP-10M accelerator in a pulse mode using the ^{3}T(p, n)^{3}He reaction to produce neutrons whereby hydrogen ion bombard a gaseous tritium target. The instrumental neutron emission spectra at a 5.74 and 4.92 MeV energy at a 45, 60, 90, 120, and 150° scattering angles, angular distributions of secondary neutrons, elastically and inelastically scattered neutron spectra, and angular distributions of inelastically distributed neutrons are plotted. The shape of the inelastically scattered neutrons virtually does not depend on the scattering angle within a 0.6-3 MeV range, attesting to the fact that the spectrum is clearly evaporative in nature. Secondary neutron spectra at a >4 MeV energy are sums of neutrons from the inelastic and elastic scattering reactions and are therefore difficult to interpret. Figures 6; references 4: 2 Russian, 2 Western.

Cosmic Ray Muon and Primary Cosmic Radiation Nucleon Intensity According to Data From Baksan Underground Scintillation Telescope

937J0003B Moscow YADERNAYA FIZIKA in Russian Vol 55 No 8, Aug 92 pp 2107-2116

[Article by V. N. Bakatanov, Yu. F. Novoseltsev, R. V. Novoseltseva, A. M. Semenov, A. Ye. Chudakov, Nuclear Research Institute at Russia's Academy of Sciences]

[Abstract] The outcome of a research program carried out at the Baksan Underground Scintillation Telescope (BPST) at the Nuclear Research Institute at Russia's Academy of Sciences (IYaI) aimed at studying the energy spectrum of cosmic ray muons and inelastic muon scattering by nuclei is discussed and corrected experimental data on the energy spectrum of cosmic ray muons as well as the muon spectrum on the surface within a 1-30 TeV range are presented. In addition, the primary cosmic radiation nucleon flux produced from the muon spectrum at an energy of 10-200 TeV/nucleon is examined. The procedure used at the BPST which is buried in rock at an $8.5 \cdot 10^{4}$ g/cm^{2} adjusted depth whereby the cascades produced by high-energy muons are measured by four horizontal scintillation planes is outlined. The muon contribution to the energy release interval, the electromagnetic cascade distribution in the zenith angle at a $\geq$111 GeV energy, and an integral energy release spectrum of electromagnetic showers are plotted. The muon intensity at the telescope depth is compared to the sea level intensity. The muon spectra in the vertical direction produced by various authors and integral muon spectra in the vertical direction according to published data are reproduced for comparison. Primary cosmic radiation (PKI) nucleon fluxes plotted by other researchers in direct experiments and by analytical means are cited. The spectrum of all primary nucleons is analyzed within a 10-200 TeV/nucleon range assuming that the superposition model is applicable. The conclusion is drawn that the spectrum of all nucleons becomes steeper up to energies on the order of 200 TeV/nucleon. Figures 6; tables 3; references 24: 9 Russian, 15 Western.

Space-Time Soliton and Dislocation Distributions in Charge Density Waves

927J0270C Moscow ZHURNAL EKSPERIMENTALNOY I TEORETICHESKOY FIZIKI in Russian Vol 102 No 1(7), Jul 92 pp 146-162

[Article by S. A. Brazovskiy, S. I. Matveyenko, Theoretical Physics Institute imeni L. D. Landau at Russia's Academy of Sciences]

[Abstract] Charge density waves (VZP) are regarded as a crystal which is characterized only by uniaxial strains from the viewpoint of the theory of elasticity and equations of the charge density waves' dissipative dynamics are derived for a continuous dislocation or soliton distribution. The problem is solved in purely dissipative CDW dynamics and in a soliton gas approximation ignoring both the possible electron diffusion before the conversion and the two-stage conversion character. The differences between the charge density wave and normal crystal dynamics are addressed and equations which describe the dynamics of both individual dislocation lines and continuous dislocation loop distribution are derived. The soliton solutions are examined and two limiting cases—solitons generated within the entire space and within a finite volume—are considered. Unidimensional charge density wave propagation in the crystal under the effect of uniform soliton generation, e.g., as a result of an electron injection by a narrow contact, and unidimensional soliton diffusion are analyzed. It is shown that the evolution of a sharp injection pulse leads to solutions which remain transient even after passing the diffusion front and the possibility of settling in a steady-state soliton current and/or concentration condition is addressed. The resulting equations cannot describe periodic oscillations accompanying the

current conversion in charge density waves because soliton aggregation into dislocations is ignored and an unlimited increase in their concentration is assumed. Figures 3; references 11: 6 Russian, 5 Western.

Steady Wave Process in Piezoelectric Layer and Half-Layer With Tunneling Slits Cutouts (Antiplane Deformation)

927J0263A Moscow PRIKLADNAYA MATEMATIKA I MEKHANIKA in Russian Vol 56 No 3, May-Jun 92 (manuscript received 23 May 91) pp 510-518

[Article by V. Z. Parton, Moscow, and M. L. Filshtinskiy, Sumy; UDC 539.3:534.1]

[Abstract] A plane-parallel piezoelectric layer and its one half-layer of a transversely isotropic material are considered, the material being a piezoceramic crystal of the 6mm hexagonal point group with the axis of symmetry parallel to the normal crystallographic z-axis (across layer thickness) and having been prepolarized parallel to this axis (x- transverse axis across layer width, y- longitudinal axis). The layer has straight or curvilinear tunneling slits of uniform width cut in its bases transversely along the path of a monochromatic electromagnetic shear wave from an infinitely distant source propagating through the layer parallel to its longitudinal y-axis. The coupling of mechanical and electromagnetic fields in such a layer results in its antiplane deformation. On the assumption that at the edges of those slits can act a harmonically alternating shear force uniformly distributed over the layer thickness parallel to the normal z-axis while both bases of the layer bounded by vacuum remain free of forces, the process of antiplane deformation is described by a complete system of equations: a) two equation relating shear stress in the xz-plane and in the yz-plane plane to z-displacement and the corresponding x,y component of the electric field, b) two equations relating the x,y components of electric induction correspondingly to the x,y components of the electric field and to normal z-displacement, c) one wave equation relating shear stresses in both xz and yz planes (sum of their x-gradient and y-gradient respectively) to normal z-acceleration, d) one equation relating rate of change of the normal (z) magnetic field to both x and y components of the electric field (x-gradient of y-component and minus y-gradient of x-component), thus allowing the problem to be reduced to electroelasticity dynamics. This system of equations with appropriate boundary conditions at the edges of the slits and the bases is solved in the quasi-static approximation, valid for small dimensions over a wide frequency range, by the methods of Green's functions and reflection (F.M. Morse and H. Feshbach) reducing it to an integrodifferential equation with a singular Hilbert kernel. This equation, with an additional constraint on displacements around slits, is then reduced to a system of linear algebraic equations. This system of equations has been solved by a numerical method (I.K. Lifanov and S.M. Belotserkovskiy) for a half-layer of PZT-4 zirconate-titanate piezoceramic with a parabolic slit. Figures 3; references 7.

Solitary Waves in Nonlinear Elastic Medium With Friction

927J0261A Minsk IZVESTIYA AKADEMII NAUK BYELARUSI: SERIYA FIZIKO- MATEMATICHESKIKH NAUK in Russian No 1, Jan-Feb 92 (manuscript received 12 Feb 90) pp 34-40

[Article by M. D. Martynenko and Nguen Dang Bik, Belorussian State University imeni V. I. Lenin; UDC 539.3]

[Abstract] Propagation of one-dimensional waves through dissipative and thus real media is analyzed for existence of solitary waves in a nonlinearly elastically deformable solid body with a stress-dependent stress-to-strain ratio s/e and with or without internal friction but with dry friction as the mechanism of energy dissipation. The analysis is based on the corresponding wave equation, the problem thus being to find what that stress dependence must be for the equation to have a solution describing solitary waves and to admit a soliton solution. This condition for existence of solitary waves in such a medium is found by considering that the stress function $s(x,t)$ must satisfy the Dodd-Eylbeck-Gibbon-Morrio equation $\delta^2 s/\delta x^2 - [K+ v(x,t)]s= 0$ and assuming that $\delta s/\delta t = Bs$ ($B= -4D^3- b_1D - b_2$, $D= d/dx$). A further analysis of this condition reveals a dependence of the propagation velocity on internal friction. When $s= b$ and $\delta s/\delta t= 0$ at $x= 0$ (origin of coordinates) at time $t= 0$ (initial condition), then solitary waves can exist in a nonlinear elastic medium with dry friction but not in one without it. Solitary waves will propagate in the positive direction or in the negative direction when $(a/\rho)^2 \geq (2c/3)^3 \leq (2c/3)^3$, $(a/\rho)^2= (2c/3)^3$ allowing for zero stress and correspondingly a width $L= D^2- v(x,t)= [-\infty,+\infty]$ (a- constant coefficient with strain rate $\delta e/\delta t$ in wave equation, ρ- density of material, 2c- propagation velocity of elastic wave). When the coefficient $a^2= \rho^{1/2}E^{3/2}/27$, then the amplitude of solitary waves does not depend on their velocity. References 2.

Nonperturbative Renormalizations and Dynamics of Breaking Electroweak Symmetries

927J0260A Kiev UKRAINSKIY FIZICHESKIY ZHURNAL in Russian Vol 36 No 12, Dec 91 (manuscript received 21 Aug 91) pp 1795-1801

[Article by V. A. Miranskiy, Institute of Theoretical Physics, UkSSR Academy of Sciences, Kiev; UDC 530.12:530.145]

[Abstract] Dynamic breaking of electroweak symmetries in two models with strong fermion-antifermion self-action is analyzed for manifestation of nonperturbative renormalizations, considering that dynamic breaking of electroweak symmetries gives rise to masses of W,Z vector bosons, quarks, and leptons. In the first model electroweak symmetries are broken through formation of a t-quark condensate, assuming a large $g_t= g^{(1)}+ g^{(3)}$ t-quark coupling constant and a small $g_b= g^{(1)}- g^{(3)}$ b-quark coupling constant. The analysis according to this

model is based on the Schroedinger-Dyson equation for the mass function of fermions in the simplest special case of $g^{(1)}= g^{(3)}$ and $g^{(2)}= 0$. When the coupling constant g_t exceeds its critical value $g_c= 1$, then the nontrivial nonzero m_t solution to this equation yields a spontaneous breaking of symmetry $U_L(2) \times U_{R(t)}(1) \times U_{R(b)}(1)$ to $U_{V(t)}(1) \times U_{L(b)}(1) \times U_{R(b)}(1)$. In the second model breaking of electroweak symmetries within the critical dynamic range leads to quark-antiquark and lepton-antilepton resonances with masses covering the 1-10 TeV range. In the case of a t-quark with sufficiently strong self-action the difficulties associated with generating masses of heavy quarks in this technicolor model can be surmounted by considering exchange of vector bosons associated with a new gauge group. The equation for the mass function of a t-quark, its right-hand side consisting of a tU-term and a tt-term, can then be treated as the Schroedinger-Dyson equation in the Nambu and Jona-Lasinio model with a bare mass. With the tt-term not disregarded, as is usually done, the solution to this equation reveals a large increase of mass owing to that strong t-quark self-action. References 32.

Coherent Spectroscopy of Raman and Hyper-Raman Light Scattering of Excited and Autoionized Atomic States in Gaseous Discharge Plasma of Copper and Copper Bromide Vapor Lasers' Active Media

937J0007A Moscow IZVESTIYA AKADEMII NAUK: SERIYA FIZICHESKAYA in Russian Vol 56 No 8, Aug 92 pp 66-75

[Article by A. M. Zheltikov, O. S. Ilyasov, A. A. Isayev, N. I. Koroteyev, Moscow State University imeni M. V. Lomonosov and International Laser Center; UDC 535.345.9]

[Abstract] The atomic component of gas discharge plasma in the active medium of Cu and CuBr vapor lasers with small H_2 additions is examined by four-photon spectroscopy and it is shown that resonances related to Raman and hyper-Raman-type scattering by excited and autoionized atomic states in the electric discharge plasma appear in the four-photon scattering spectra. The experimental unit is described and the active hyper-Raman and Raman scattering spectroscopy procedures are outlined. The polarization properties of the coherent anti-Stokes light scattering (KARS) signal under resonance conditions at an anti-Stokes emission frequency and active Raman scattering spectroscopy of autoionized Cu atom states are investigated in detail. The population and decay kinetics of electronic excited states of atoms in electric discharge plasma are examined and the correlations between the hyper-Raman scattering tensor invariants of excited atomic states are determined on the basis of experimental polarization measurements. The autoionized states of Cu atoms in discharge plasma are established and Fano's parameters are determined by comparing the four-photon process spectrum at the frequency of transitions between the excited and autoionized states to the calculated data. Figures 5; tables 1; references 25: 18 Russian, 7 Western.

Pulse Signal Polarization Plane Rotation Dynamics in GaAs Crystal: Single- and Double-Photon Absorption

937J0007B Moscow IZVESTIYA AKADEMII NAUK: SERIYA FIZICHESKAYA in Russian Vol 56 No 8, Aug 92 pp 95-106

[Article by M. G. Dubenskaya, T. M. Ilinova, A. V. Trukhov, A. A. Fortygin, Department of Physics and International Laser Center at the Moscow State University imeni M.V. Lomonosov; UDC 621.315.592]

[Abstract] The effect of light polarization self-action also known as nonlinear optical activity (NOA) and its phenomenological theory and uses are discussed and an attempt is made theoretically to analyze the phenomenon of nonlinear optical activity related to the nonlinear absorption anisotropy developing under one- and two-photon impulse excitation of a direct gap A^3B^5 semiconductor. The cubic susceptibility tensors near the absorption band edge are analyzed in the framework of a double-gap semiconductor model with a spherically symmetric conduction band and crumpled (or corrugated) heavy hole valence band. The cubic susceptibility tensor and pulse signal polarization plane rotation under a one-photon resonance as well as the cubic susceptibility tensor and pulse signal polarization rotation under a two-photon resonance are examined in detail. The findings indicate that under a two-photon resonance, the corrugated valence band shape is the principal cause of the nonlinear absorption anisotropy in GaAs; in the case of a one-photon resonance, the carrier distribution function skewness must also be taken into account. Moreover, under a one-photon resonance, the medium's cubic polarization depends on the current pulse energy due to the integral population accumulation effect under slow relaxation. Formulae describing the pulse signal's polarization characteristics are derived. Figures 1; references 9: 7 Russian, 2 Western.

Nonlinear Spectroscopy of Ultrafast Structural Organic Molecule Dynamics Processes

927J0270A Moscow ZHURNAL EKSPERIMENTALNOY I TEORETICHESKOY FIZIKI in Russian Vol 102 No 1(7), Jul 92 pp 47-58

[Article by V. F. Kamalov, Yu. P. Svirko, Chemical Physics Institute at Russia's Academy of Sciences and General Physics Institute at Russia's Academy of Sciences]

[Abstract] Structural dynamics of organic molecules are considered using the example of *trans*-stilbene photoisomerization and the use of active Raman scattering spectroscopy (ASKR) with a femtosecond time resolution which opens up new possibilities for examining ultrafast structural dynamics processes is discussed. An attempt is made to demonstrate the expediency of using E.J. Heller's approach to describing the nonlinear resonance scattering of ultrashort light pulses by means of active Raman scattering spectroscopy and assess the outlook for its applications for studying the optical radiation relaxation with a characteristic time on the order of the electron excitation dephasing time. The relative advantages of two experimental designs of the resonant active Raman scattering spectroscopy method are examined from this viewpoint and a simple model is developed for describing the wave packet evolution in the excited electron state. The wave depolarization degree at the anti-Stokes frequency is calculated on the basis of this model. It is noted that within the range of characteristic times used, all Raman scattering oscillations of the electron's ground state contribute to the active Raman scattering hyperpolarization of the molecule. The authors are grateful to Drs. H. Hamaguchi, K. Yoshihara, and H. Okamoto for assistance. Figures 2; references 18: 2 Russian, 16 Western.

Double Optical Resonance in Semiconductor Quantum Well

927J0274A St. Petersburg PISMA V ZHURNAL TEKHNICHESKOY FIZIKI in Russian Vol 18 No 11, Jun 92 pp 9-11

[Article by V. A. Sinyak, Applied Physics Institute at the Moldovan Academy of Sciences, Chisinau; UDC 01; 06.3; 0.7]

[Abstract] The unique properties of quantum wells and superlattices and their optoelectronic applications are discussed and the interband absorption of weak light by a semiconductor quantum well with infinite walls under the effect of a powerful electromagnetic wave at a frequency less than the forbidden gap width whereby the electromagnetic wave propagates perpendicular to the well plane is considered ignoring the intraband absorption. The charge carrier wave functions in the powerful electromagnetic wave field defined by the vector potential are derived in the effective mass approximation. After manipulations, absorptance of the GaAs-$Ga_{1-x}Al_xAs$ quantum well as a function of the weak light frequency is derived. References 3: 1 Russian, 2 Western.

On Nonlinear Intensity Fluctuations of Light Pulse Transmitted Through Semiconductor Layer

927J0278A St. Petersburg PISMA V ZHURNAL TEKHNICHESKOY FIZIKI in Russian Vol 18 No 9, May 92 pp 6-10

[Article by Yu. N. Karamzin, S. V. Polyakov, V. A. Trofimov; UDC 07]

[Abstract] The report presented to the 14th International Conference on Coherent and Nonlinear Optics held in St. Petersburg in September 1991 is reprinted in full. The issue of the buildup of the output light pulse intensity fluctuations at a constant input value in optical bistability experiments realized in a semiconductor crystal is addressed and an attempt is made to demonstrate the possibility of periodic output intensity conditions in optical radiation transmitted through a semiconductor and focused on the rear face of the crystal in the case where the electron excitation and relaxation dynamics as a function of temperature are significant and are taken into account. The light beam interaction with the semiconductor crystal is described by a system of nondimensional equations with known initial boundary value conditions and a formula is derived for the dependence of absorptance on the electron concentration and temperature. The output signal intensity fluctuation, temperature, and electron concentration dynamics in the crystal at a constant input intensity, and phase portraits of these processes are plotted. The new class of periodic output light pulse intensity fluctuations after transmission through a semiconductor crystal is not related to the earlier observed relaxation oscillations in optical bistability problems; it is speculated that the incorporation of thermal generation of charge carriers even where the recombination time does not depend on temperature will lead to similar processes. Figures 2; references 6: 4 Russian, 2 Western.

Nonlinear Light Absorption in Exciton Resonance Region in Semiconductor Heterostructure Self-Quantized Layers (Multilayer Heterostructure With Self-Quantized Layers)

927J0264A Yerevan IZVESTIYA AKADEMII NAUK ARMENII: SERIYA FIZIKA in Russian Vol 26 No 2, Mar-Apr 91 pp 61-66

[Article by A. G. Aleksanyan, Al. G. Aleksanyan, G. S. Nikogosyan, Radio Physics and Electronics Institute at the Armenian Academy of Sciences; UDC 621.373.5]

[Abstract] Interest in the studies of various nonlinear processes in multilayer semiconductor heterostructures (MG) with self-quantized layers (KRS) is noted and absorption saturation in a multilayer semiconductor heterostructures with self-quantized layers due to the shielding of the electron's and hole's Coulombian interaction by the nonequilibrium carriers is considered. A formula is derived for absorptance allowing for the exciton effects and Elliott's factor in this formula S is computed allowing for the Coulombian interaction screening by nonequilibrium carriers using Yukawa's screened Coulomb potential. In particular, Elliott's factor is calculated with the help of an approximate solution of Schroedinger's equation with Yukawa's potential. An analysis shows that saturation phenomena in GaAs-AlGaAs multilayer semiconductor heterostructures with self-quantized layers occurs at a lower intensity than in a bulk GaAs semiconductor due to their higher absorptance which is determined by the state density effect and the Coulombian interaction enhancement. Moreover, absorptance decreases monotonically to the interband absorptance level within the entire increasing radiant intensity range. The findings are consistent with the published experimental absorption data. References 6: 2 Russian, 4 Western.

Power Fluctuation Statistics of Optical Radiation Scattered in Turbulent Atmosphere

927J0264B Yerevan IZVESTIYA AKADEMII NAUK ARMENII: SERIYA FIZIKA in Russian Vol 26 No 2, Mar-Apr 91 pp 101-103

[Article by A. V. Oganesyan, Physical Research Institute at the Armenian Academy of Sciences; UDC 621.396]

[Abstract] The importance of knowing the power fluctuation statistics of the optical radiation scattered in the turbulent atmosphere for optimizing the detection of optical ranging signals prompted an attempt to derive the power fluctuation probability density of the optical radiation scattered in the turbulent atmosphere. A situation is considered where a spotted structure of the optical field in the detection plane with real a collecting

aperture is defined primarily by scattering and turbulence leads to a change in the total mean illuminance level. Thus, statistical power fluctuations of the detected radiation are examined in the case where the collecting aperture radius is smaller than the coherence radius and the receiving aperture encompasses many independent coherent regions of the scattered optical field. The probability density curve of the optical signal power fluctuation is plotted. Figures 1; references 4: 2 Russian, 2 Western.

On Effect of Optical Cell Wall on Excited Atomic State Relaxation and Light Polarization

937J0001A St. Petersburg OPTIKA I SPEKTROSKOPIYA in Russian Vol 72 No 2, Feb 92 pp 271-275

[Article by V. N. Rebane, T. K. Rebane, St. Petersburg State University; UDC 539.183.01]

[Abstract] The anisotropic relaxation of angular momenta of excited atomic states whereby the effect of collisions on the atomic ensemble is axisymmetric and differs from that of isotropic relaxation is discussed and an attempt is made to demonstrate that anisotropic relaxation of the excited atomic states is also realized in the case where the emitting particles do not collide with the particles of the ambient gaseous media but are present near the optical cell or cavity wall. This premise is illustrated by the example of an atomic ion in an excited state located near the optical cell wall. It is shown that the anisotropic excited state relaxation is due to the splitting of the degenerate ion energy level under the effect of the electrostatic image forces. This relaxation leads to a collisionless linear light polarization transition to circular polarization. The circular polarization signal condition is similar to anisotropic collisions; it peaks when the exciting light vector slope is equal to 45° to the anisotropy axis. The findings can be extended to the case of higher orbital and spin electron shell momenta and to the case of neutral atomic particle interaction with the cell wall; in this case all the main features of the problem remain unchanged. References 11: 2 Russian, 9 Western.

Determining CO Molecule $a^3\pi$-State Excitation Function With Electron Impact

937J0001B St. Petersburg OPTIKA I SPEKTROSKOPIYA in Russian Vol 72 No 2, Feb 92 pp 276-279

[Article by A. A. Markov, M. A. Khodorkovskiy, A. I. Dolgin, Scientific Production Association of the State Applied Chemistry Institute, St. Petersburg; UDC 539.196:546.262]

[Abstract] The excitation function of carbon monoxide molecule's (CO) metastable $a^3\Pi$ state by an electron impact and the low accuracy of optical measurements of metastable state cross sections are discussed and an attempt is made to determine the excitation function of the metastable $a^3\Pi$ state of the CO molecule from the threshold to the 50 eV level by the method of time-of-flight spectroscopy in intersecting electron and gas dynamic beams. A schematic diagram of the experimental unit used for this purpose is cited and its design and operating principle are explained. A VEU-1A secondary electron multiplier is used as the metastable particle detector. The low work function (4 eV) of the first aluminum dynode made it possible to record the $a^3\Pi$ state at a 6 eV energy. The time-of-flight spectrum of the CO molecule and and the CO molecule $a^3\Pi$ state excitation function are plotted. A discrepancy between the authors' experimental results and other data in the area of >25 eV is attributed to a decrease in the effect of cascade transitions and secondary electrons due to a hundredfold decrease in the gas pressure in the electron beam interaction area. The findings demonstrate the advantages of time-of-flight metastable spectroscopy using supersonic molecular beams. The time-of-flight method also makes it possible to measure not only the excitation cross sections but also to estimate the lifespans of the excited states. Figures 2; references 7: 3 Russian, 4 Western.

Effect of Monochromatic Excitation Frequency on Collision Transitions Between Hyperfine Atomic Levels

937J0001C St. Petersburg OPTIKA I SPEKTROSKOPIYA in Russian Vol 72 No 2, Feb 92 pp 280-289

[Article by A. G. Petrashen, V. N. Rebane, T. K. Rebane, St. Petersburg State University; UDC 539.186.3]

[Abstract] New phenomena in polarization optics caused by the relaxation of excited toms under anisotropic particle collisions are discussed and it is noted that the theory of these phenomena is outpacing experimental research in this field. The anisotropic collisional relaxation of an atomic ensemble excited by monochromatic light of a unimodal laser is examined theoretically under the collisions of excited particles possessing a rigidly defined velocity projection along the light beam with the ambient gaseous medium particles whose velocities have a stochastic Maxwellian distribution. For illustration, three typical experimental situations are considered in the case where the 3/2 level is selectively excited by monochromatic light. The signal of sensitized fluorescence emitted by the hyperfine ½ level under the excitation of the 3/2 hyperfine level by a monochromatic light pulse, the effect of the hyperfine 3/2 level ordering and laser frequency detuning on the collisional population transport from the 3/2 to the ½ level, the dependence of the signal peak delay of sensitized fluorescence emitted from the ½ level on the laser frequency detuning, and the ratio of the time-sensitive ½ and 3/3 hyperfine level populations are plotted. The anisotropic collisional relaxation matrix elements of the ^{113}Cd atom's hyperfine structure as a function of the laser frequency detuning from the Doppler line center are calculated. The findings indicate that the collision population transport process

rate can be controlled by manipulating the laser frequency; this is also true for the fine structure levels of narrow thin multiplets. Figures 4; tables 1; references 23: 14 Russian, 9 Western.

Collision Breakup of Ar4$s(^3P_2)$ Metastable Atoms in He-Ar Mixture

937J0001D St. Petersburg OPTIKA I SPEKTROSKOPIYA in Russian Vol 72 No 2, Feb 92 pp 290-292

[Article by V. A. Ivanov, I. V. Makasyuk, A. S. Prikhodko, St. Petersburg State University; UDC 539.186.2]

[Abstract] Heightened interest in elementary processes involving inert gas atoms in metastable states and the lack of thorough data on the collision behavior of the Ar4$s(^3P_2)$+He system prompted an attempt to measure the k_{He} quenching rate constant of Ar4$s(^3P_2)$ metastable atoms under collisions with He atoms. A low current pulse discharge in a He-Ar mixture with a low Ar concentration filling a glass tube with a 0.6 cm radius and 30 cm length is used as the metastable Ar atom formation source while rate constant data are obtained by analyzing the dependence of the density drop rate in the afterglow on the He atom density at various electron concentrations. The Ar states density decrease as a function of time and the dependence of the Ar atom metastable state breakup frequency in decaying plasma on the He pressure and initial electron concentration are plotted. The process has an intermediate stage whereby the 3/2 resonant state is excited and a resonant quantum is emitted. The experiment demonstrates for the first time the rate constant of the Ar 3/2 $\rightarrow$3/1 transitions in a He-Ar mixture stimulated by collisions of metastable atoms with helium atoms. At a gas temperature of 300K, the rate constant is equal to $2.1+/-0.2\cdot10^{-15}$ cm^3/s. Figures 3; references 8: 6 Russian, 2 Western.

Breakup of Ar4$s(^3P_0)$ Metastable Atoms by Thermal Electrons

937J0001E St. Petersburg OPTIKA I SPEKTROSKOPIYA in Russian Vol 72 No 2, Feb 92 pp 293-295

[Article by V. A. Ivanov, I. V. Makasyuk, St. Petersburg State University; UDC 539.186.2]

[Abstract] The importance of examining the processes involving excited atoms in metastable states for understanding the phenomena occurring in various plasma entities and the lack of experimental data on the destruction of metastable atoms in argon plasma prompted an attempt to measure the rate of Ar4$s(^3P_0)$ destruction by thermal electrons in plasma. The study is carried out in weakly ionized decaying He-Ar plasma with a <1 percent Ar concentration; the advantages of using this mixture rather than the afterglow plasma in pure Ar are outlined. The drop in the states density of argon and electron concentration as a function of time and the dependence of the metastable state destruction frequency in decaying plasma on the initial electron concentration as well as the Ar4s configuration level arrangement are plotted. An analysis of the experimental results makes it possible to calculate the destruction rate constant: at a 300K temperature, it is equal to $2.6+/-0.2\cdot10^{-7}$ cm^3/s. It is noted that the findings are not sufficient for determining the channel of the electron destruction/recombination population reaction. Figures 3; references 7: 6 Russian, 1 Western.

New Types of Diffraction Switching Waves and Autosolitons in Nonlinear Interferometers

937J0001F St. Petersburg OPTIKA I SPEKTROSKOPIYA in Russian Vol 72 No 2, Feb 92 pp 447-453

[Article by N. N. Rozanov, State Optics Institute imeni S.I. Vavilov, St. Petersburg; UDC 35.2+535.4]

[Abstract] Diffraction autosolitons—particle-like field structures in wide-aperture nonlinear interferometers excited by radiation with a radially uniform intensity distribution—which differ in principle from the diffusion autosolitons and solitons observed when an interferometer with sharp mirror edges is excited by a bounded beam are discussed and an attempt is made to produce new types of diffraction autosolitons (DAS) and diffraction switching waves (DVP) in bistable and multistable interferometers in the framework of an analytical approach which treats diffraction autosolitons as the bounded state of diffraction switching waves. Analytically, both are constructed for model nonlinearity. The model and the initial relationships are formulated and the bistability and multistability cases are examined. The transverse intensity distribution in a wide-aperture interferometer is plotted for the switching waves and diffraction autosolitons under both bistability and multistability conditions. Altogether, combined DVP (a DVP coupled with one or several DAS), moving asymmetric DAS (bound combined DVP), and bound DVP (two ordinary DVP) are demonstrated. The DAS and DVP represent a new class of dynamical conditions of particle-like field structures in a wide-aperture nonlinear interferometer; conditions in an interferometer with distributed properties in both transverse dimensions are even more diverse. The use of moving structures is promising for all-optical processor applications. Figures 2; references 11: 8 Russian, 3 Western.

Correlation Properties of Scattered Coherent Radiation Within Wide Range of Illumination and Observation Conditions

937J0001G St. Petersburg OPTIKA I SPEKTROSKOPIYA in Russian Vol 72 No 2, Feb 92 pp 474-478

[Article by L. A. Glushchenko, I. A. Popov, State Optics Institute imeni S.I. Vavilov, St. Petersburg; UDC 535.36]

[Abstract] The limited applicability of the model of delta-correlated inhomogeneities of a scattering rough surface widely used in speckle pattern analysis prompted an attempt to derive an asymptotic expression for the correlation function of radiation scattered by a linearly moving surface with a normal inhomogeneity distribution law in the domain of Kirchhoff's procedure applicability using the steepest descent method. The study demonstrates that the resulting approximation corresponds to the delta-correlation model and makes it possible to find its applicability criteria. General expressions are derived for the correlation function of scattered radiation within a broad range of illumination and observation parameters in the free space geometry and for an optical projection system. The applicability conditions call for a sufficiently large size of the illuminating beam or the scattering circle of the projection system relative to the irregularity size. The role of the illuminating beam wave front's radius of curvature is identified and the field space and time correlation properties are analyzed for a nonGaussian scattered radiation function. References 8: 2 Russian, 6 Western.

Contactless Diffraction Method of Measuring Angular Displacements and Vibrations of Reflecting Surfaces

937J0001H St. Petersburg OPTIKA I SPEKTROSKOPIYA in Russian Vol 72 No 2, Feb 92 pp 479-486

[Article by V. A. Komotskiy, V. F. Nikulin, University of the Friendship Among Nations imeni Patrice Lumumba, Moscow; UDC 535.39]

[Abstract] The importance of contactless measurement methods in today's science, especially experimental physics, prompted an investigation into a new method of contactless recording of small angular displacements and vibrations of reflecting surfaces which has never been described in published sources yet has a number of valuable advantages over known methods. The method is based on double interaction of the optical beam with a diffraction grating. An optical train of the method is cited and the measurement procedure is outlined in detail. The experimental unit consists of a laser, a diffraction grating, a diaphragm, and a photodetector; the output signal is defined as the voltage on the photodetector load. The experimental dependence of the output voltage on the angular displacement of the reflecting object and the dependence of the output voltage slope and peak-to-peak amplitude as well as the arithmetic mean of the output voltage on the distance between the diffraction grating and the reflecting surface are plotted. The limit of resolution and dynamic measurement range are calculated allowing for the laser beam divergence. The proposed system is suitable for examining membrane vibrations within a broad range of frequencies, for detecting long surface acoustic waves propagating on the surface of solids and liquids, and for detecting standing waves on the liquid surface. It is suggested that the method be tested for determining the deformation of solids due to photothermal and photoacoustic effects. Figures 3; references 5.

Expanding Bragg's Diffraction Selectivity Bandwidth Using Optically Active Crystals

937J0009A Kiev UKRAINSKIY FIZICHESKIY ZHURNAL in Russian Vol 37 No 2, Feb 92 pp 261-265

[Article by L. F. Kupchenko, Yu. V. Astashev, A. M. Reznichenko, I. N. Goltvyanskiy; UDC 621.391:535.33]

[Abstract] The effect of the Bragg diffraction selectivity on limiting the analyzed bandwidth of optoacoustic spectral analyzers and the optical radiation deflection angle of optoacoustic scanners and the issue of expanding this bandwidth are addressed. Earlier findings (Zilberman, Kupchenko *et al*) resulting in analytical expressions of this type of diffraction are further developed and an attempt is made to demonstrate that in optically active uniaxial crystals, two Bragg synchronism conditions (which obtain under anisotropic Bragg diffraction) determined by the presence of optical activity exist in addition to the ordinary and extraordinary refractive indices. To this end, it is shown that both Bragg's principal and additional conditions can be found from known formulae assuming that the nonreciprocity parameter is equal to zero. Light diffraction on an ultrasonic grating in a uniaxial optically active crystal is considered and the Bragg diffraction selectivity in the regions of low and high ultrasonic frequencies is examined. The study indicates that by using joint light diffraction with ordinary Bragg's angles and the angles determined by optical activity, one can expand the bandwidth of spectral analyzers. It is suggested that optically active crystals with a sufficiently high component of the gyration tensor be used as the acoustic line material to expand the frequency selectivity bandwidth of Bragg's diffraction provided that the interaction conditions are met. Formulae are derived for the angles ensuring the bandwidth expansion. Figures 2; references 7.

On Possibility of Determining Spatial Plasma Oscillation Spectrum by Enhanced Microwave Scattering Method

927J0275C St. Petersburg PISMA V ZHURNAL TEKHNICHESKOY FIZIKI in Russian Vol 18 No 10, May 92 pp 63-66

[Article by Ye. Z. Gusakov, A. D. Piliya, Engineering Physics Institute imeni A.F. Ioffe at Russia's Academy of Sciences, St. Petersburg; UDC 01; 04; 09]

[Abstract] The use of enhanced scattering—an efficient method of investigating small-scale plasma oscillations whereby plasma is probed by an electromagnetic wave for which the upper hybrid resonance condition is met inside the plasma while the radiation scattered by the plasma at a close to 180° angle is recorded—is discussed and attention is focused on the possibility of improving the method's resolution by using a modulated pump wave. To this end, plasma probing by a sequence of short pulses and by a frequency-modulated probing wave is considered and it is noted than in real experiments, frequency fluctuations are not monochromatic. The analytical formulae are modified for this factor and the modification is shown to be suitable for analyzing narrow quasimonochromatic plasma oscillation spectra which are characteristic of low hybrid waves in RF heating and entrainment current generation experiments. References 2: 1 Russian, 1 Western.

Magnetic Ordering and Phase Separation in High-T_c Superconductors

937J0004A Moscow TEORETICHESKAYA I MATEMATICHESKAYA FIZIKA in Russian Vol 92 No 2, Aug 92 pp 344-352

[Article by A. N. Yermilov, Mathematics Institute imeni V.A. Steklov at Russia's Academy of Sciences]

[Abstract] The role of magnetism in CuO_2 plane-based high-T_c superconductors and the hypothesis that electron pairing in HTSC is closely related to magnetic excitations are discussed and an attempt is made to examine magnetic ordering in copper oxides at a moderate impurity concentration and investigate the phase separation in $La_2CuO_{2+\delta}$ using the Monte Carlo method. The general structure of the HTSC phase diagram is plotted in the temperature vs. impurity concentration coordinates and the underlying premises of the Monte Carlo model developed for analyzing the magnetic properties are formulated. It is assumed that the impurity ion induces the hole in the CuO_2 plane, that at moderate temperature the hole is coupled with the impurity ion and localized on the plane region containing several oxygen ions, and that the hole located on the oxygen ion on the plane changes the antiferromagnetic coupling between the spins of the adjacent copper ions to ferromagnetic coupling. The factors underlying these assumptions are examined in detail. The modifications to the underlying assumptions necessary for explaining the phase separation are formulated and it is shown that defective nests have a clear tendency toward clustering. Since the nest centers are excess oxygen ion positions, this indicates the formation of domains with a low and high oxygen concentration or phase separation. The phase separation process is described quantitatively and the conclusion is drawn that clustering and phase separation are due to a frustration energy gain. Figures 5; references 34: 6 Russian, 29 Western.

Superconductivity in Systems With Strong Electron-Phonon Coupling

927J0270B Moscow ZHURNAL EKSPERIMENTALNOY I TEORETICHESKOY FIZIKI in Russian Vol 102 No 1(7), Jul 92 pp 132-145

[Article by A. Ye. Karakozov, Ye. G. Maksimov, A. A. Mikhaylovskiy, Physics Institute imeni P. N. Lebedev at Russia's Academy of Sciences]

[Abstract] The excitation spectra and dynamic properties of superconductors with strong coupling are discussed and it is noted that thus far, little attention has been given to this issue due to the need to know the solutions of Eliashberg's equations on the real axis of variable energy. The electron-phonon coupling is represented in the form of a sum of regular and singular components and Eliashberg's equations are analyzed for systems with such strong coupling. A model spectral function and the solution of the coupling equation are plotted and the energy gap and electron states density in a superconductor with strong electron-phonon coupling is considered; the regular part of the electron-phonon coupling is plotted. The solution of Eliashberg's integral equation in the form of regular and singular components is close to the Bardeen-Cooper-Schrieffer model coupling which is convenient for analyzing and numerically solving the equations directly on the real axis; in addition, the density of states at finite temperatures differs from zero at all energies as a result of which there are excitations in the superconductor spectra with the energies falling within the energy gap. In the limit of large coupling constants (i.e., much higher than unity), the energy gap has $\lambda^{1/2}\omega$ asymptotics at $T=0$. The authors are grateful to O.V. Dolgov, D.A. Kirzhnits, A.L. Lesnikov, and S.V. Shulga for discussions and assistance. Figures 7; references 19: 4 Russian, 15 Western.

Study of Josephson's Effect in Weakly Coupled High-T_c Superconductors Using Microwave Scanner

927J0274C St. Petersburg PISMA V ZHURNAL TEKHNICHESKOY FIZIKI in Russian Vol 18 No 11, Jun 92 pp 31-34

[Article by V. F. Masterov, A. V. Prikhodko, G. G. Selmistraytis, A. N. Chursinov; UDC 05.4; 09]

[Abstract] The lack of Josephson effect studies using the differential microwave (SVCh) methods prompted an attempt to demonstrate the possibility of investigating high-T_c superconductors (VTSP) using the differential technique; it is based on using the principle of scanning the sample's *XY*-plane by the microwave radiation lobe of a dielectric antenna. The relatively small scanning area volume makes it possible to avoid the purely technical difficulties related to the contact selection and to carry out the experiment by simulating the physical parameters in a single sample. The experimental procedure is described and the voltage-current characteristic of the sample at 77 and 300K and the dependence of the current detected by the sample on the 30 GHz microwave power incident upon the sample without biasing (modulated at a 100 Hz frequency) are plotted. The results obtained in weakly coupled Y-Ba-Cu-O ceramics show that the voltage-current curve is resistive at 300K but a Josephson current segment is observed at a 77K temperature; generally, it cannot be detected by stationary methods. In the absence of external stress and microwave exposure, an inverse Josephson effect is observed at 77K, i.e., microwave radiation is detected by the internal Josephson junctions. The dependence of the detected current on the system position relative to the grounded sample end is especially noteworthy due to the nonmonotonic current dependence which is attributed to the sample nonuniformity. The proposed method can be used to determine the homogeneity of a multiple Josephson medium, such as ceramic HTSCs. The authors are grateful to L.V. Knishevskaya. The effort is supported by the Scientific Council on the HTSC Problem in the framework of project No. 90418. Figures 2; references 5: 4 Russian, 1 Western.

Protection of High-Current HTSC-Metal Contacts Using Controlled Live Element Texturing

927J0275B St. Petersburg PISMA V ZHURNAL TEKHNICHESKOY FIZIKI in Russian Vol 18 No 10, May 92 pp 21-25

[Article by A. Yu. Volkov, A. A. Bush, S. N. Gordeyev, Obninsk Nuclear Power Engineering Institute and

Moscow Radio Engineering, Electronics, and Automation Institute; UDC 05.4; 12]

[Abstract] The importance of developing the technology of low-resistance mechanically strong current contacts for high-T_c (VTSP) superconductor elements both for practical and research applications is noted and the need to protect the contacts from thermal loads, contact failure, and ceramic electrolysis is stressed. A new approach to protecting high-current contacts of HTSC elements which takes into account the characteristics of the HTSC materials is developed and it is suggested that the near-contact segments from a HTSC material with higher critical parameters be formed while fabricating the contacts. The protection method is based on the well-known dependence of critical HTSC parameters on the texturing axis duration and degree during the production of samples by the floating zone melting method with optical heating (OZP). To check the theory of controlled texturing with the help of floating zone melting with optical heating, an experiment is conducted; the potential difference distribution between pairs of potential contacts at various transport currents, the position of potential and current contacts on the sample, and the rate of growth of the contact segments during the OZP texturing are plotted. An analysis demonstrates that the of controlled texturing makes it possible to protect high-current HTSC element contacts which must be able to pass to the normal state and back from overheating. Figures 1; references 13: 8 Russian, 5 Western.

Degradation of Ceramic Y-123 and Bi(Pb)-2223 Superconductors Stimulated by Exposure to Gamma Radiation

927J0261B Minsk IZVESTIYA AKADEMII NAUK BYELARUSI: SERIYA FIZIKO- MATEMATICHESKIKH NAUK in Russian No 1, Jan-Feb 92 (manuscript received 12 Jul 91) pp 41-44

[Article by F. P. Korshunov, L. F. Makarenko, V. K. Shesholko, I. F. Kononyuk, L. V. Makhnach, N. M. Olekhnovich, O. I. Pashkovskiy, and V. D. Yanovich, Institute of Solid-State and Semiconductor Physics, Byelorusian Academy of Sciences; UDC 538.945]

[Abstract] An experimental study of ceramic Y-123 and Bi(Pb)-2223 superconductors was made concerning their resistance to gamma radiation, dependence of that resistance on the technological parameters, and the mechanisms of their degradation by radiation treatment and electron bombardment. Higher-density (5.8-6.0 g/cm^3) Y-123 ceramic with better mechanical characteristics was obtained by inclusion of an annealing at 990-1020°C in an oxygen atmosphere and subsequent slow cooling cycle in the sintering process, its critical superconducting transition temperature then being T_{c0}= 92.5-92.8 K and its critical current density varying over the 250-350 A/cm^2 range. Specimens of Bi(Pb)-2223 ceramic were produced from three different materials: grade Bi52 ($Bi_{1.65}Pb_{0.35}Sr_{1.9}Ca_{2.1}$ Cu_3O_y, grade Bi18($Bi_{1.8}Pb_{0.3}$ $Sr_2Ca_2Cu_3O_y$, grade Bi72 ($Bi_{1.8}Pb_{0.4}Sr_2Ca_2Cu_3$ O_y. Some specimens were irradiated with gamma quanta up to about $1.5x10^{18}$ cm^{-2} (10^9 R) from a Co-60 source and others were bombarded with 4 MeV electrons up to $1.5x$ 10^{18} cm^{-2}. The temperature dependence of their electrical resistance and their critical transport current density at 77 K (liquid nitrogen) were measured by the standard current-voltage method. The data reveal that there is an optimum temperature for synthesis of these ceramics, a higher temperature favoring formation of other phases and particularly the tetragonal one with a resulting degradation of the superconductor characteristics (lower critical temperature and critical current) and especially so by subsequent especially after electron bombardment. The results of this study indicate that degradation of their superconductor characteristics by gamma radiation superposes on and thus enhances their degradation due to thermochemical aging, the rate of degradation then depending on the composition of the atmosphere in which these ceramics have been irradiated as well as on the amounts of water vapor and carbon dioxide they have absorbed prior to irradiation. Figures 2; references 14.

Certain Methods in Nonlinear Regression Analysis

927J0275A St. Petersburg PISMA V ZHURNAL TEKHNICHESKOY FIZIKI in Russian Vol 18 No 10, May 92 pp 6-10

[Article by A. A. Galickas, Semiconductor Physics Institute at the Lithuanian Academy of Sciences, Vilnius; UDC 01; 12]

[Abstract] The convenience of using nonlinear mathematical models for describing most physical phenomena and the lack of a general and efficient regression analysis procedure for this purpose prompted an attempt to develop general computational techniques which facilitate the convergence of the computational process. The principal premises of the regression analysis methods are formulated and the procedures of observation point randomization, linear stage identification, and iteration calculation are considered. The results of a numerical computer realization of the methods using a specific physical model containing seven parameters three of which are nonlinear are discussed. For this purpose, 100-250 observation points are selected and convergence is achieved and optimum parameters calculated in only 5-20 iterations which take one to three minutes on an IBM PC/AT microcomputer without a math coprocessor at a clock frequency of 12 MHz. The proposed methods ensure a three- to fivefold better convergence than the Gauss-Newton procedure. Analysis of a 12-parameter model with eight nonlinear variables is reported. References 4.

Optimization of Estimates of Spatially Distributed Parameters in Electrodynamic Models of Surfaces in Inverse Interpretation Problems During Active Telemetry

927J0277A Moscow DOKLADY AKADEMII NAUK SSSR in Russian Vol 322 No 2, Jan 92 (manuscript received 21 Nov 91) pp 277-280

[Article by V. K. Volosyuk, V. F. Kravchenko, and S. Ye. Falkovich, Scientific Research Institute of Precision Instruments, Moscow, and Kharkov Institute of Aviation; UDC 537.874.4]

[Abstract] A solution of inverse problems of parameter estimation in active telemetry is proposed for parameters $\lambda(\rho)$ characterizing a surface $\rho(x,y)$, the recorded field $U_{kl}(r,t)$ being described by a system of nonlinear integral equations of the second kind: U_{kl} (r,t) equal to real parts of integrals over surface D plus a noise n_{kl} (r,t) (r- radius vector, t- time). The integrand function F[dot over $F]_{kl}[\rho,\lambda(\rho),r]$ is generated by boundary conditions and known from the solution to the corresponding problem of wave scattering for a given electrodynamic model of surface D. The kernel S[dot over $S]_{0l}(r,\rho,t)$ is determined by the geometry of measurements and the waveform of transmitted coherent signals. The subscripts l= (v,h) and kl= (vv,vh,hv,hh) characterize the polarization mode of transmitted and received signals (v- vertical, h- horizontal). The random noise n_{kl} (r,t) represents recording errors with a correlation function R_n $(r_1,r_2,t_1,t_2)= (N_{0kl}/2)\delta(r_1- r_2)\delta(t_1- t_2)$. The optimum estimates of function $\lambda(\rho)$ are based on zero first variational derivatives of the corresponding likelihood functionals. The integrand virtually ceases to be a function of r and becomes simply F[dot over $F]_{kl}[\rho,\lambda(\rho)]$ when the dimensions of the field recording region are much smaller than the altitude of its location above the target surface, whether it is located within the far field or the near field relative to the signal scatterers. The kernel S[dot over $S]_{0l}(r,\rho,t)$ should then be treated as the reference signal for primary processing of the $U_{kl}(r,t)$ field. As practical examples are considered a geometry of measurements suitable for static holography, a stationary field recording region, and a moving system of lateral scan with a synthetic aperture. In the last case the system of integral equations for the recorded field and the corresponding system of likelihood equations together describe optimum nonlinear filtration, their left-hand sides describing a special kind of optimum discriminator for primary processing of the recorded field U_{kl}. A special discriminator is required for primary processing which involves involves including in the structure of the reference an electrodynamic model F[dot over $F]_{kl}$, a function or r or t, based on scattering of electromagnetic waves by surface D. References 6.

NTIS
ATTN PROCESS 103
5285 PORT ROYAL RD
SPRINGFIELD VA 22161

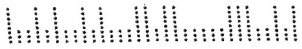

Foreign Broadcast Information Service (FBIS) and Joint Publications Research Service (JPRS) publications contain political, military, economic, environmental, and sociological news, commentary, and other information, as well as scientific and technical data and reports. All information has been obtained from foreign radio and television broadcasts, news agency transmissions, newspapers, books, and periodicals. Items generally are processed from the first or best available sources. It should not be inferred that they have been disseminated only in the medium, in the language, or to the area indicated. Items from foreign language sources are translated; those from English-language sources are transcribed. Except for excluding certain diacritics, FBIS renders personal names and place-names in accordance with the romanization systems approved for U.S. Government publications by the U.S. Board of Geographic Names.

Headlines, editorial reports, and material enclosed in brackets [ ] are supplied by FBIS/JPRS. Processing indicators such as [Text] or [Excerpts] in the first line of each item indicate how the information was processed from the original. Unfamiliar names rendered phonetically are enclosed in parentheses. Words or names preceded by a question mark and enclosed in parentheses were not clear from the original source but have been supplied as appropriate to the context. Other unattributed parenthetical notes within the body of an item originate with the source. Times within items are as given by the source. Passages in boldface or italics are as published.

SUBSCRIPTION/PROCUREMENT INFORMATION

The FBIS DAILY REPORT contains current news and information and is published Monday through Friday in eight volumes: China, East Europe, Central Eurasia, East Asia, Near East & South Asia, Sub-Saharan Africa, Latin America, and West Europe. Supplements to the DAILY REPORTs may also be available periodically and will be distributed to regular DAILY REPORT subscribers. JPRS publications, which include approximately 50 regional, worldwide, and topical reports, generally contain less time-sensitive information and are published periodically.

Current DAILY REPORTs and JPRS publications are listed in *Government Reports Announcements* issued semimonthly by the National Technical Information Service (NTIS), 5285 Port Royal Road, Springfield, Virginia 22161 and the *Monthly Catalog of U.S. Government Publications* issued by the Superintendent of Documents, U.S. Government Printing Office, Washington, D.C. 20402.

The public may subscribe to either hardcover or microfiche versions of the DAILY REPORTs and JPRS publications through NTIS at the above address or by calling (703) 487-4630. Subscription rates will be provided by NTIS upon request. Subscriptions are available outside the United States from NTIS or appointed foreign dealers. New subscribers should expect a 30-day delay in receipt of the first issue.

U.S. Government offices may obtain subscriptions to the DAILY REPORTs or JPRS publications (hardcover or microfiche) at no charge through their sponsoring organizations. For additional information or assistance, call FBIS, (202) 338-6735,or write to P.O. Box 2604, Washington, D.C. 20013. Department of Defense consumers are required to submit requests through appropriate command validation channels to DIA, RTS-2C, Washington, D.C. 20301. (Telephone: (202) 373-3771, Autovon: 243-3771.)

Back issues or single copies of the DAILY REPORTs and JPRS publications are not available. Both the DAILY REPORTs and the JPRS publications are on file for public reference at the Library of Congress and at many Federal Depository Libraries. Reference copies may also be seen at many public and university libraries throughout the United States.